A STUDY OF THE AIR EJECTOR

THESIS

Submitted in Partial Fulfilment of the Requirements

for

the Degree of Master of Engineering

by

ALAN G. LANE

McGILL UNIVERSITY
MONTREAL, QUEBEC

AUGUST 1950

PREFACE

The experimental research for this paper was performed under the auspices of the Mechanical Engineering Department of McGill University, in the Gas Dynamics Laboratory at Montreal. The author wishes to express his appreciation to all the members of this department who have helped and contributed in this work, and in particular to the Chairman of the department and the Defence Research Board who have provided the necessary funds for the construction of the apparatus.

The author is also greatly indebted to Prof. D. L. Mordell, who initially suggested the topic of investigation and under whose direction the research was performed, for his unfailing guidance throughout the work. The assistance and frequent advice of the colleagues, and the use of the Departmental Machine Shop for the fabrication of the equipment has been appreciated at all times.

Chapter 3 of this paper has been reproduced with permission, in its entirity, from a report submitted earlier by the author in the course of studies.

Alan G. Lane, B.Eng.

August 1950

CONTENTS

LIST OF ILLUSTRATIONS

LIST OF TABLES

NOMENCLATURE

The following will be used uniformly throughout this paper.

A – Area in ft^2

C_p – Specific heat at constant pressure in ft.pdls./lb.°R value 6060 for air at N. T. P.

D – Diameter at section specified.

L – Length of mixing section.

m – Mass flow in lbs./sec.

$\bar{m}$ – Ratio of mass flows = m_3 / m_1

p – Static pressure in pdls./ft^2

P – Total pressure (of stagnation) in pdls./ft^2

R – Gas constant in ft.pdls./lb.°R (1718 for air)

t – Static temperature of air (i.e. relative to observer moving with stream) in °R

T – Total temperature (of stagnation) in °R

u – Local velocity in axial (x) direction

U – Principal stream velocity in ft./sec.

v – Local velocity in transverse (y) direction

V – Principal stream velocity in ft./sec.

x – Longditudinal distance in mixing region.

y – Transverse distance in mixing region.

β – Index = $\frac{\gamma - 1}{\gamma}$

γ – Ratio of specific heats = C_p/C_v

η – Adiabatic efficiency, also a parameter.

ρ – Fluid density in pdls./ ft^3

Subscripts used in the text refer to sections as defined on page 4.

SUMMARY

A brief review of the contemporary investigations of Keuthe, Keenan, Neumann and others is presented and forms the basis for enlargement of the theory to cover more cases than in the past. A general momentum equation is introduced which is adaptable to either constant area or constant pressure mixing and more generally to all cases of constant pressure gradient mixing. The author's experimental work substantiates this theory and shows that the losses for any one geometrical design are approximately a constant proportion of the relative dynamic head.

The theory for the turbulent mixing of free jets is derived and applied to find the divergence angle for a jet into a parallel flow. In addition the length required for complete mixing is determined both analytically and experimentally, and the results agree favourably.

Investigations of the discontinuities occurring in the mixing section indicate that oblique shock waves distribute themselves in order to reduce the velocity for a subsonic diffusion to the discharge conditions.

Recommendations are made for design, and possible performance characteristics may be predicted within a reasonable margin of accuracy. It is emphasised however, that the scale effect of model test ejectors eliminates their use for experimental determination of full size ejector operation and capacities.

CHAPTER 1

Introduction

The ejector consists primarily of a pump in which a jet of fluid at high velocity entrains another fluid surrounding it and forces the mixture through a discharge tube. In order to obtain this high velocity jet the fluid for this purpose must be expanded from a relatively high pressure through a nozzle to some pressure suitably below the discharge pressure. The induced, or "secondary" fluid, on the other hand, which enters the mixing region at this same pressure, is compressed by the process up to the discharge pressure.

The earliest forms of ejectors were designed to use steam as the " primary" or activating fluid since this could be easily obtained at high pressures, and expanding nozzles had been previously designed for this medium. Applications of this steam ejector were in locomotive and small stationary plant feed pumps and water pump evacuators. Later high pressure water was used as the primary fluid to extract or pump other liquids and gases in commercial fields. At the present time both forms of the ejector are widely used, and in a few instances special types are employed with gas as both primary and secondary media, however the majority of designs have been arrived at by a trial and error process and their performance is not entirely reliable.

Although much analytical work was done by Prandtl[15]* and Tollmien[19] in 1925 on the turbulent mixing of jets with a secondary medium, the experimental verification was concerned with the mixing of free jets in still air.

---

* Superscripts denote references in bibliography.

The first recorded tests of mixing in a confined region were by Watson[22] in 1933, in which the results were shown for the evacuation of a tank by means of a steam ejector. The conclusions drawn from this work were unfortunately limited by the specific conditions involved and do not admit to universal application.

Later investigations by Flügel (1939)[8] Keenan, Neumann (1942)[14] and others found it suitable to consider separately the cases of constant area and constant pressure mixing; on the assumption that an ideal design would be obtained either near to one of these conditions, or between them. Flügel obtained a series of formulae adaptable to each specific case by a system of subdivision according to the media and type of mixing. Keenan and Neumann in their paper, were more concerned with the geometric design and sought an optimum length for the mixing section and optimum angles for convergence and divergence to and from a constant area mixing tube.

The contemporary papers of Forstall[9] and Baron[2] have been based on an even further generalization of the turbulent mixing of jets as applied to free and restricted mixing regions regardless of media. These however, are proposed more for the purpose of jet-propulsion ducts and thrust augmentation and contain no experimental results of ejectors as such.

It is the purpose of this paper to present a further consideration of the important formulae, developing a more general formula than those of references 8 and 14, and to apply these in conjunction with reference 19 to determine mixing lengths and other variables in terms of the parameters of the ejector. These variables will be further explained in the following chapter.

CHAPTER 2

The General Analysis

A cross-section of the typical ejector is shown in Figure 1, in which the primary fluid is expanded from high pressure resevoir conditions 0 to its exit from the nozzle 1. Simultaneously the secondary fluid is expanded from 2 to 3, at which point the two streams are assumed to meet at the same static pressure. The mixing process continues in the passage 3 to 4, and the completely mixed fluids are then diffused to condition 5.

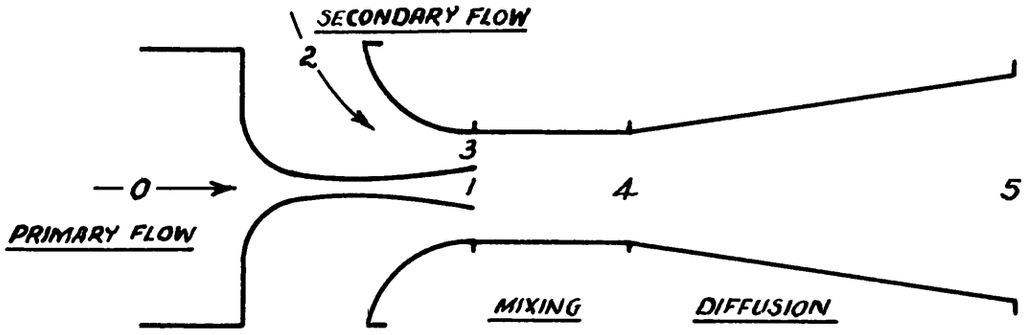

FIG. 1* — CROSS-SECTION OF EJECTOR

Throughout the analysis it will be found convenient to limit the consideration initially to the case of identical fluids for which the gas constant R, and specific heats C_p and C_v - and therefore γ and β are the same. It will be seen later that the theory may be extended to include other cases as they arise without materially altering the solutions achieved.

The expansion in both activating and induced nozzles may be reduced with the use of an assumed adiabatic efficiency η, to the following:

---

*Note. Figure 1 is reproduced on the last page, and may be folded out for reference.

$$\frac{V_1^2}{2C_pT_1} = \eta_{01}\left[1 - \left(\frac{p_1}{p_0}\right)^{\beta}\right] \qquad [1]$$

and

$$\frac{V_3^2}{2C_pT_3} = \eta_{23}\left[1 - \left(\frac{p_3}{p_2}\right)^{\beta}\right] \qquad [2]$$

Further if the discharge velocity is relatively small compared with V_4, the expression for diffusion is

$$\left(\frac{p_5}{p_4}\right)^{\beta} = 1 + \frac{\eta_{45} V_4^2}{2C_pT_4} \qquad [3]$$

There remains the intermediate mixing process which has intentionally been retained to this point, and over which much speculation has been raised. Fundamentally the equations of continuity

$$m_1 + m_3 = m_4 \qquad [4]$$

and energy

$$m_1T_1 + m_3T_3 = m_4T_4 \qquad [5]$$

may be written, assuming a constant specific heat at constant pressure within the mixing region.

The general equation of momentum for the mixing process may be deduced from Figure 2, as

$$p_1(A_1 + A_3) + m_1V_1 + m_3V_3 + \int_{A_1+A_3}^{A_4} p.dA = p_4A_4 + m_4V_4 \qquad [6]$$

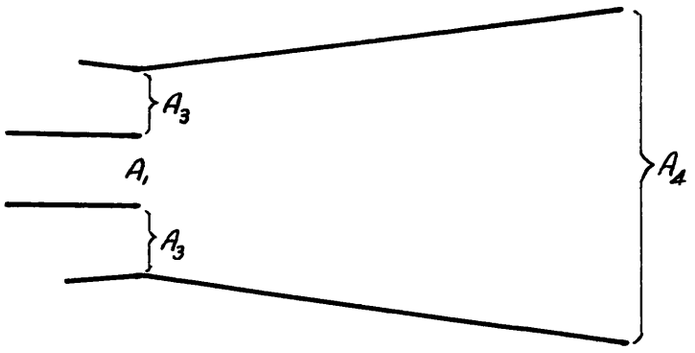

FIG. 2 - DIVERGENT MIXING SECTION

The integral represents the axial (i.e. "x" component) of the wall thrust due to change of profile. The evaluation of this integral greatly complicates the analysis except in the following three cases.

Constant Pressure Mixing

In this case $p_1 = p_3 = p_4$ and thus

$$\int_{A_1+A_3}^{A_4} p.dA = p_1 \ (A_4 - A_1 + A_3) \qquad [7]$$

and equation [6] reduces to

$$m_1V_1 + m_3V_3 = m_4V_4 = (m_1 + m_3)\ V_4 \qquad [8]$$

indicating that in this process, where the initial velocities are equal, they remain unchanged upon mixing. Alternatively, if the velocities, mass flows and pressure at inlet are known, the exit velocity V_4 may be calculated by means of the above equation, and the area A_4 may be determined from the relationship

$$m = \rho AV = \frac{pAV}{Rt} \qquad [9]$$

where

$$t = T - \frac{V^2}{2C_p} \qquad [10]$$

The value of V_4 may be substituted in equation [3] to find the ratio P_5/p_4 and hence the induction pressure ratio,

$$\frac{P_2}{P_5} = \frac{P_2}{p_3} \times \frac{p_4}{P_5}$$

$$= \left[1 - \frac{V_3^2}{2C_p \eta_{23} T_2}\right]^{-1/\beta} \left[1 + \frac{\eta_{45} V_4^2}{2C_p T_4}\right]^{-1/\beta} \qquad [11]$$

Constant Area Mixing

Although this form is mechanically simple, and indeed the integral of equation [6] reduces to zero, since there can be no wall thrust, the same equation becomes,

$$1 - \frac{R}{2C_p} V_4^2 - \left[\frac{p_1 A_4 + m_1 V_1 + m_3 V_3}{m_1 + m_3}\right] \cdot V_4 + RT_4 = 0 \qquad [12]$$

This quadratic yields the solutions for V_4, from which p_4 may be found in equations [9] and [10]. The remainder of the procedure is similar to that for the constant pressure case.

Constant Gradient Mixing

Since in the majority of ejectors manufactured to date the mixing section comprises a ruled surface (i.e. conical or cylindrical) it is reasonable to postulate a case in which the static pressure gradient within the region is constant, as well as the area gradient. For this case,

$$\int_{A_1+A_3}^{A_4} p.dA = \frac{p_3 + p_4}{2} \left\{A_4 - \overline{A_1 + A_3}\right\} \qquad [13]$$

It will be noted that on specifying the conditions of constant pressure

or constant area mixing, the solution reduces to the same values given previously, namely:

$$\text{Const. Press.} \quad \int p.dA = p_1 \left(A_4 - \overline{A_1 + A_3}\right)$$

$$\text{Const. Area} \quad \int p.dA = 0$$

Upon substituting the value of the integral from [13] into the momentum equation, a quadratic results for V_4, as

$$\left[\frac{A}{2C_p} - 1\right] V_4^2 + \left[\frac{2A \left(p_1 A/2 + m_1 V_1 + m_3 V_3 \right)}{R \left(m_1 + m_3 \right)}\right] . V_4 - AT_4 = 0 \qquad [14]$$

where "A" is twice the mean cross-sectional area of the mixing tube,

$$A = A_4 + A_3 + A_1 .$$

The solution for p_4 and hence P_2/P_5 are again as outlined for the constant pressure case. It appears that this solution is more general than either of its predecessors and can be employed for nearly all simple ejector designs.

Mixing Length

The former analysis has lead to a development of the area ratio necessary for complete mixing of the streams. From this divergence it is possible to calculate the length of duct required for complete mixing by two methods.

The first is naturally to assume some optimum angle of divergence usually about 4 or 5 degrees, and hence obtain the length required to effect this increase of cross-section. However since the performance of the ejector itself is still a matter of question it is also doubtful that the same angles used for a diffusion process would apply equally

well in all situations, to turbulent mixing.

The alternative method is to apply the theory of turbulent mixing of free jets to obtain this angle, and by this means, calculate the length of mixing section. The following chapter is devoted entirely to this aspect of the problem.

CHAPTER 3

Turbulent Mixing of Free Jets

The turbulent mixing region of a free jet may be considered as analagous to the case of turbulent boundary layer in simple flow, in regard to the mixing length and boundary conditions. Figure 3, below illustrates a jet at velocity U_1 entering a region of still air, that is, with no velocity parallel to U_1.

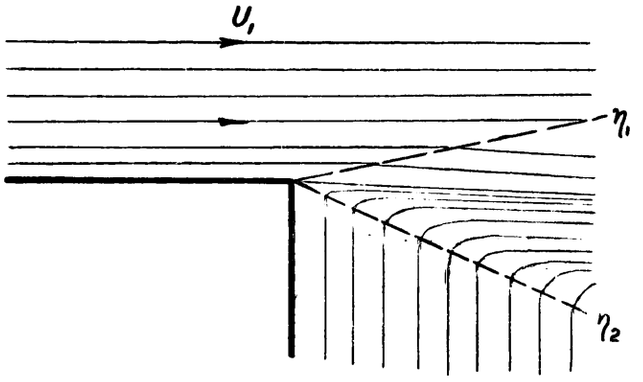

FIG. 3
JET ISSUING INTO STILL AIR

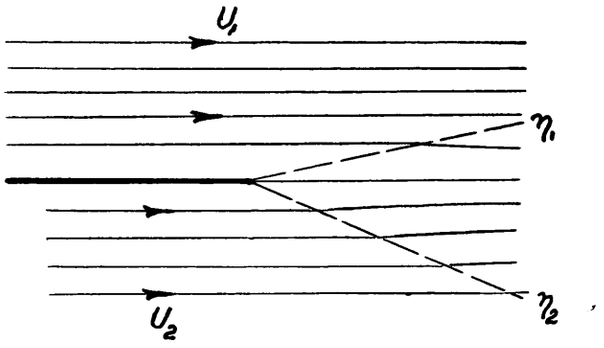

FIG. 4
MIXING OF TWO PARALLEL FLOWS

This case was first investigated by Tollmien* in 1926, but it will be observed that this is only one particular condition for the mixing of parallel flows. The more general case, is illustrated in Fig. 4 in which U_1 is the main stream velocity, and U_2 is the velocity of the entrained fluid. On the basis that this flow is similar to the conditions encountered in boundary layer theory, it is reasonable to postulate that there are two planes, η_1 and η_2 at which the uniform velocity is disturbed

---

* W. Tollmien "Berechnung turbulenter Ausbreitungsvorgange" - Zeitschrift fur Angewandte Mathematik und Mechanik, Band 6, Heft 6, 1926, p. 468

and turbulent mixing commences.

Assuming that the main stream velocity U_1 in the x-direction is a function of y only, and that ℓ, the mixing length -- the distance between layers of momentum change -- is constant across a cross-section, and is proportional to the breadth of the mixing zone, then the principal shear stress is

$$\tau_{xy} = \rho \ell^2 \left(\frac{\partial u}{\partial y}\right) \left|\frac{\partial u}{\partial y}\right| \qquad [1]$$

Prandtl* proves that it is reasonable to assume that the pressure gradients in both the axial and transverse directions are negligable, and further assuming steady state conditions, the first equation of motion becomes

$$u \frac{\partial u}{\partial x} + v \frac{\partial v}{\partial y} = \frac{1}{\rho} \frac{\partial}{\partial y} \tau_{xy} \qquad [2]$$

The continuity equation then is,

$$\frac{\partial u}{\partial x} + \frac{\partial v}{\partial y} = 0 \qquad [3]$$

Then since $u \cdot dy - v \cdot dx$ is a perfect differential equal to ψ say, ψ is a stream function such that

$$u = \frac{\partial \psi}{\partial y} \quad \text{and} \quad v = -\frac{\partial \psi}{\partial x} \qquad [4]$$

Futher, if

$$u = f(y/x) \quad \text{and} \quad y/x = \eta \quad \text{say,} \qquad [5]$$

then it follows that

$$\psi = \int u \cdot dy = \int f(y/x)\, dy = x\, F(\eta) \text{ say,}$$

from which

$$\begin{aligned} u &= \frac{\partial \psi}{\partial y} = F' \\ v &= -\frac{\partial \psi}{\partial x} = -F + \eta F' \end{aligned} \qquad [6]$$

---

* L. Prandtl "Bericht uber Untersuchungen zur ausgebildeten Turbulenz"

Since the mixing length is assumed proportional to x we may put

$$\ell = c.x$$

where c is some constant, and substitute in equation [2] to obtain

$$-\frac{y}{x^2} F' F'' + \left[-F + \eta F'\right] \frac{1}{x} F'' = \frac{1}{\rho} \cdot \frac{\partial}{\partial y} \left[\rho c^2 x^2 \left(\frac{\partial u}{\partial y}\right)^2 \right]$$

which reduces to

$$\left.\begin{aligned} F + 2c^2 F''' &= 0 \\ \text{or} \qquad F'' &= 0 \end{aligned}\right\} \qquad [7]$$

the latter giving the upstream undisturbed conditions. The former may be written as

$$F + F''' = 0 \qquad [8]$$

where $$\eta = \frac{1}{\sqrt[3]{2c^2}} \frac{y}{x}$$

It is found preferable to use a system of coordinates which expresses the distance from the upper boundary $\eta' = \eta - \eta_2$. Then the general solution for equation [8] as given by Murray* reduces to

$$F(\eta') = \alpha_1 \varepsilon^{-\eta'} + \alpha_2 \varepsilon^{\eta'/2} \cos \frac{\sqrt{3}}{2} \eta' + \alpha_3 \varepsilon^{\eta'/2} \sin \frac{\sqrt{3}}{2} \eta' \qquad [9]$$

This equation determines the mixing region in terms of the five unknowns α_1 α_2 α_3 η_1 and η_2 . Four of these may be eliminated by the boundary conditions; at the upper surface where the jet begins to mix, η_1 , that is where $u = U_1$; and at the lower surface η_2 ($\eta' = \eta_2'$) , where $u = U_2$. In both cases

$$\left.\begin{aligned} \frac{\partial u}{\partial y} &= 0 \\ \frac{\partial u}{\partial \eta'} &= 0 \end{aligned}\right\}$$

---

* D. A. Murray "Differential Equations" - Longmans and Green 1945, p. 64

The fifth boundary condition was chosen by Tollmien as $v_1 = 0$ at $\eta' = 0$, that is at the η_1 boundary, which applies to an expansion into free air at $U_2 = 0$. However Kuethe* extends this particular case to include $u_2 = U_2$ by using the momentum relationship,

$$u_1 . v_1 = - u_2 . v_2 \qquad [10]$$

which is merely applying Newton's law to the reaction across a plane parallel to the jet. Across this plane, naturally the action and reaction are equal and opposite. It may further be shown that this assumption does not affect the width of the mixing region nor the u-velocity profiles since it is independant of η_1 and η_2. A summary of the boundary conditions then follows;

At the inside boundary where $\eta = \eta_1$; $\eta' = 0$ and $u = U_1$

$$\left.\begin{array}{rcl} u\eta_1 = F(\eta') & & U_1\eta_1 = F(0) \\ u = F'(\eta') & & U_1 = F'(0) \\ \frac{u}{\eta'} = F''(\eta') & & 0 = F''(0) \end{array}\right\} \qquad [11]$$

At the outside boundary where $\eta = \eta_2$; $\eta' = \eta_2'$ and $u = U_2$

$$\left.\begin{array}{rcl} u\eta_2 = F(\eta_2') & & U_2\eta_2 = F(\eta_2') \\ u = F'(\eta_2') & & U_2 = F'(\eta_2') \\ \frac{u}{\eta_2'} = F''(\eta_2') & & 0 = F''(\eta_2') \end{array}\right\} \qquad [12]$$

The momentum equation [10] also becomes,

$$U_2 \left[-F(\eta_2') + \eta_2 F'(\eta_2')\right] = U_1 \left[F(0) - \eta_1 F'(0)\right] \qquad [13]$$

Then equation [9] and its three derivatives are,

---

* A. M. Kuethe "Investigations of the turbulent mixing regions formed by Jets" - Transactions of the American Society of Mechanical Engineers 1935, vol. 57, Journal of Applied Mechanics pp A-87 to A-95.

$$\left.\begin{aligned}
F(\eta') &= \alpha_1\varepsilon^{-\eta'} + \alpha_2\varepsilon^{\eta'/2}\cos\tfrac{\sqrt{3}}{2}\eta' + \alpha_3\varepsilon^{\eta'/2}\sin\tfrac{\sqrt{3}}{2}\eta' \\
F'(\eta') &= -\alpha_1\varepsilon^{-\eta'} + \left(\tfrac{\alpha_2}{2} + \tfrac{\alpha_3\sqrt{3}}{2}\right)\varepsilon^{\eta'/2}\cos\tfrac{\sqrt{3}}{2}\eta' + \left(\tfrac{\alpha_3}{2} - \tfrac{\alpha_2\sqrt{3}}{2}\right)\varepsilon^{\eta'/2}\sin\tfrac{\sqrt{3}}{2}\eta' \\
F''(\eta') &= \alpha_1\varepsilon^{-\eta'} + \left(\tfrac{\alpha_3\sqrt{3}}{2} - \tfrac{\alpha_2}{2}\right)\varepsilon^{\eta'/2}\cos\tfrac{\sqrt{3}}{2}\eta' - \left(\tfrac{\alpha_3}{2} + \tfrac{\alpha_2\sqrt{3}}{2}\right)\varepsilon^{\eta'/2}\sin\tfrac{\sqrt{3}}{2}\eta' \\
F'''(\eta') &= -\alpha_1\varepsilon^{-\eta'} - \alpha_2\varepsilon^{\eta'/2}\cos\tfrac{\sqrt{3}}{2}\eta' - \alpha_3\varepsilon^{\eta'/2}\sin\tfrac{\sqrt{3}}{2}\eta'
\end{aligned}\right\} \quad [14]$$

Now on putting the conditions of [11] into equations [14] it is possible to solve for the constants α_1 α_2 α_3 as,

$$\alpha_1 = \frac{U_1}{3}(\eta_1 - 1)$$

$$\alpha_2 = \frac{U_1}{3}(1 + 2\eta_1)$$

$$\alpha_3 = \frac{U_1}{\sqrt{3}}$$

The conditions [12] give, for the outside boundary,

$$\left.\begin{aligned}
U_2\eta_2 &= \alpha_1\varepsilon^{-\eta_2'} + \alpha_2\varepsilon^{\eta_2'/2}\cos\tfrac{\sqrt{3}}{2}\eta_2' + \alpha_3\varepsilon^{\eta_2'/2}\sin\tfrac{\sqrt{3}}{2}\eta_2' \\
U_2 &= -\alpha_1\varepsilon^{-\eta_2'} + \left(\tfrac{\alpha_2}{2} + \tfrac{\alpha_3\sqrt{3}}{2}\right)\varepsilon^{\eta_2'/2}\cos\tfrac{\sqrt{3}}{2}\eta_2' + \left(\tfrac{\alpha_3}{2} - \tfrac{\alpha_2\sqrt{3}}{2}\right)\varepsilon^{\eta_2'/2}\sin\tfrac{\sqrt{3}}{2}\eta_2' \\
0 &= \alpha_1\varepsilon^{-\eta_2'} + \left(\tfrac{\alpha_3\sqrt{3}}{2} - \tfrac{\alpha_2}{2}\right)\varepsilon^{\eta_2'/2}\cos\tfrac{\sqrt{3}}{2}\eta_2' - \left(\tfrac{\alpha_3}{2} + \tfrac{\alpha_2\sqrt{3}}{2}\right)\varepsilon^{\eta_2'/2}\sin\tfrac{\sqrt{3}}{2}\eta_2'
\end{aligned}\right\} \quad [15]$$

Then between these equations and the values of the constants we obtain

$$\bar{U} = \varepsilon^{\eta_2'/2}\left[\cos\tfrac{\sqrt{3}}{2}\eta_2' - \frac{2\eta_1+1}{\sqrt{3}}\sin\tfrac{\sqrt{3}}{2}\eta_2'\right] \quad [16]$$

where

$$\bar{U} = \frac{U_2}{U_1}$$

and

$$\eta_1 = \frac{1}{\frac{\sqrt{3}}{\tan\frac{\sqrt{3}}{2}\eta_2'} + 1} \quad [17]$$

Hence by taking values of $\bar{U}$ between unity and zero, it is possible to find corresponding values of η_2' which provide the solutions to equations [14]

for the remaining unknowns. These values are then entered below in Table 1. Since these values are determined without the use of the condition $u_1 v_1 = - u_2 v_2$ they correspond to the Tollmien assumption that $v_1 = 0$ at the inside jet boundary. However on equating between [13] and [15] a slightly different set of values are obtained for η_1 and η_2 as shown in Table 1, introducing this momentum equation.

TABLE 1 - Values of constants α and η_1 η_2

$\bar{U}$	$\frac{\alpha_1}{U_1}$	$\frac{\alpha_2}{U_1}$	$\frac{\alpha}{U_1}$	η_2'	$v_1 = 0$		$u_1 v_1 = - u_2 v_2$	
					η_1	η_2	η_1	η_2
0	-0.0062	0.987	0.577	-3.020	0.981	-2.040	0.981	-2.040
0.1	-0.012	0.976	0.577	-2.773	0.962	-1.811	0.934	-1.839
0.2	-0.020	0.960	0.577	-2.565	0.940	-1.625	0.905	-1.660
0.4	-0.038	0.924	0.577	-2.190	0.885	-1.305	0.850	-1.340
0.6	-0.067	0.866	0.577	-1.821	0.797	-1.024	0.783	-1.038
0.8	-0.117	0.766	0.577	-1.380	0.647	-0.733	0.645	-0.735
0.9	-0.159	0.682	0.577	-1.080	0.522	-0.558	0.523	-0.557
1.0	-0.333	0.333	0.577	0	0	0	0	0

The values of η_1 and η_2 for both these methods are plotted in Fig. 5 on the next page, and show the close correlation between the two assumptions. Figure 6 is a graph of the velocity distribution for various values of $\bar{U}$, showing in a more pictorial manner the results of the theory.

At this point it should be remembered that an early transformation was made from y/x to η which involved the constant c. This factor must be determined experimentally since it governs the actual velocity profile, and two values have so far been obtained;

Kuethe, $c = 0.0174$ Forthmann*, $c = 0.0165$

Using the mean of these values, $c = 0.0170$ it is then possible to construct

---

* E. Forthmann "Uber turbulente Strahlausbreitung" Ingenieur-Archiv, Band 5, Heft 1, 1934, pp 42-54.

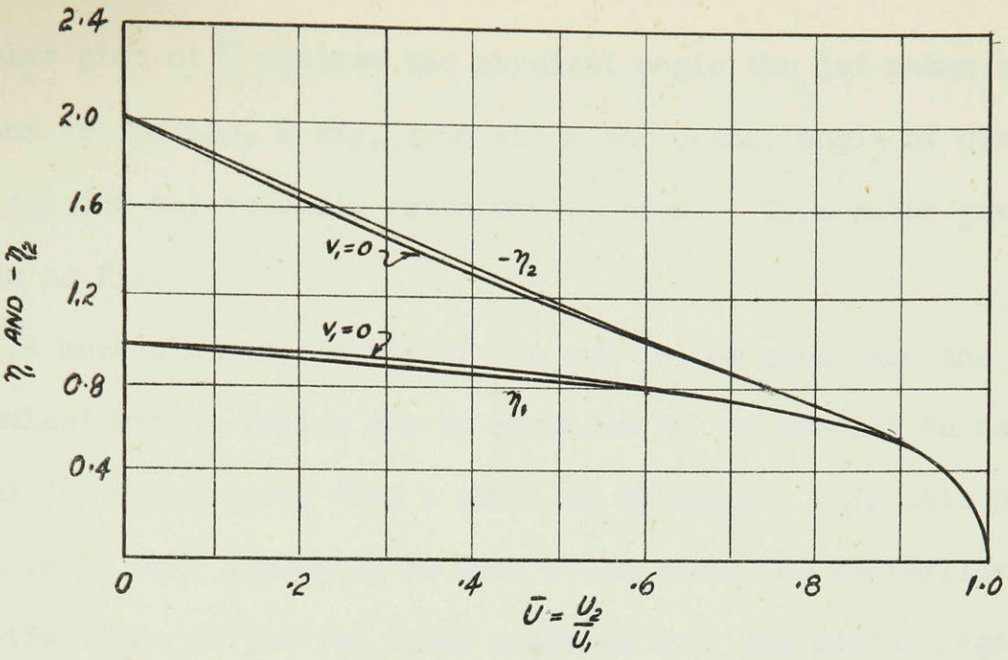

FIG. 5 - GRAPH OF η_1 AND $-\eta_2$ VS. $\bar{U}$

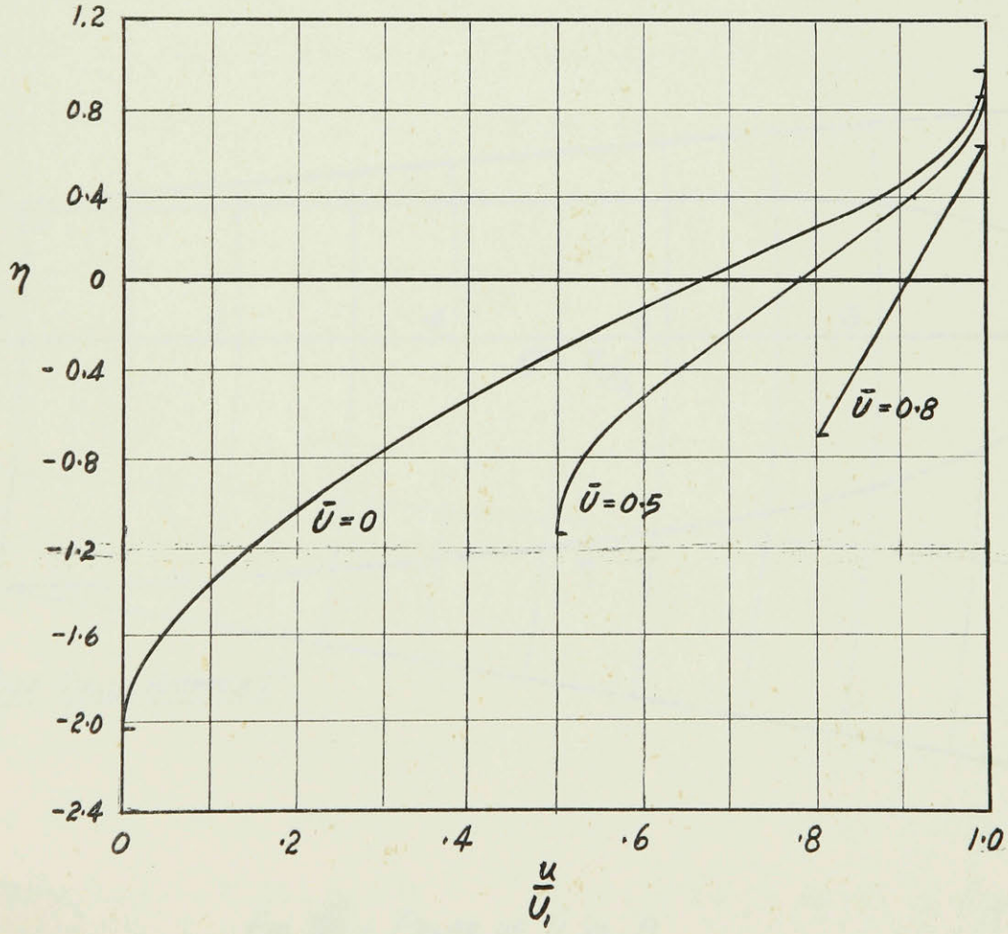

FIG. 6 - VELOCITY PROFILE FOR THREE VALUES OF $\bar{U}$

a polar plot of $\bar{U}$ against the physical angle the jet makes with the main stream velocities, θ say, from which the actual angle of divergence of the jet for any velocity ratio may be seen. This polar graph is submitted below as Fig. 7.

A much clearer picture of the jet is now seen, and the theory of the turbulent mixing region may be extended to the case of an axially symetrical jet discharging from a parallel cylinder. In this particular case there will evidently be some point along the centerline at which the original core of the jet fluid vanishes into the mixing region. This point e on Fig. 8 is taken as the limit of the initial mixing stage A, and the beginning of a more complex turbulent stage B in which the irregularities are assumed to smooth out, up to the plane at f, from

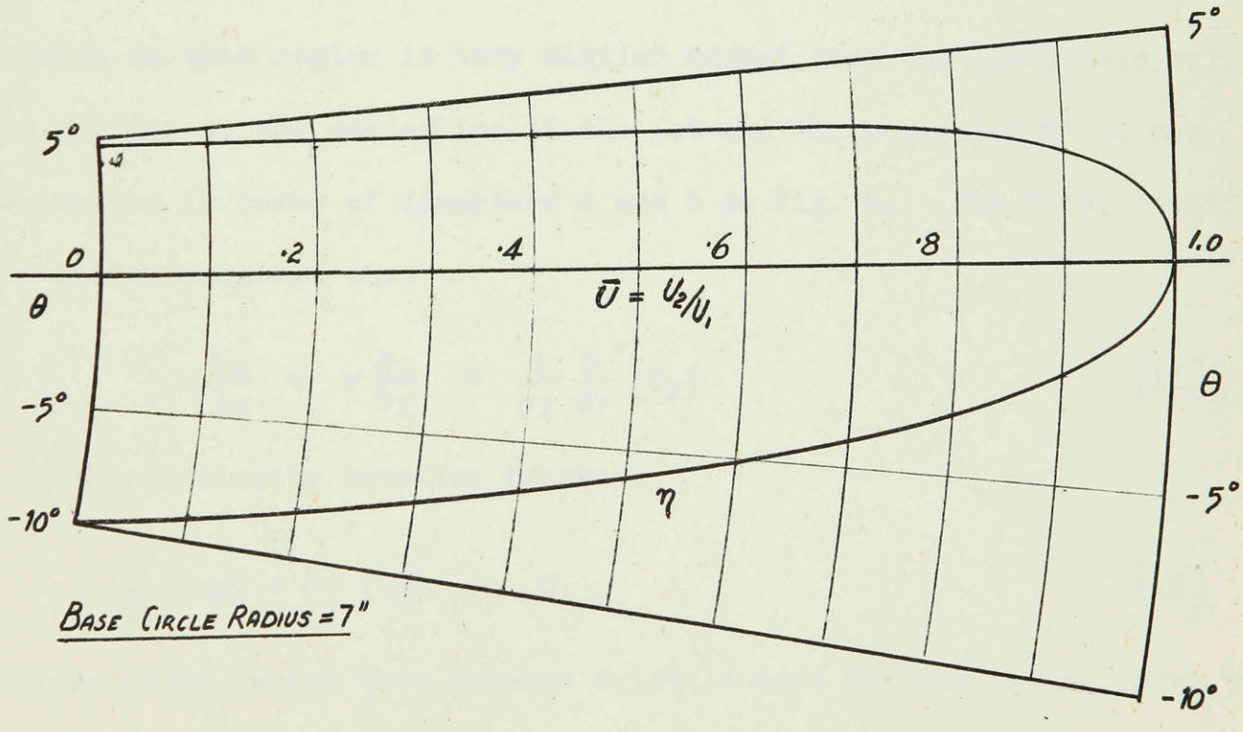

Fig. 7 - Polar of $\bar{U}$ vs. θ

$$\theta = \tan^{-1}(\eta \sqrt[3]{2c^2})$$

which point on the velocity profile remains relatively unchanged.

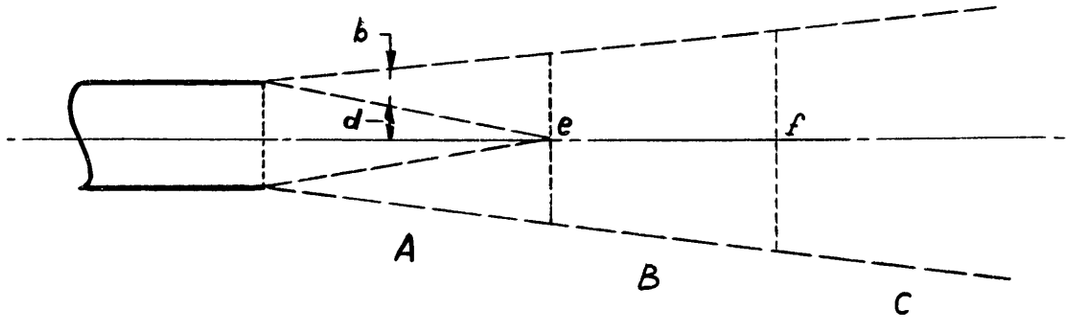

FIG. 8 – AXIALLY SYMETRICAL JET.

In the analysis of an ejector, the region A is of primary importance since the region B will likely be governed in its outside boundary by the walls of the mixing space. The mathematical treatment of the turbulent mixing in this region is very similar except that the coordinate origin is shifted to the centerline of the jet and the parameter η' is now expressed in terms of diameters d and b on Fig. 8. The first equation of motion requires that

$$u \frac{\partial u}{\partial x} + v \frac{\partial u}{\partial y} = \frac{1}{\rho y} \frac{\partial}{\partial y} (\tau y) \qquad [18]$$

and the continuity equation becomes,

$$\frac{\partial}{\partial x} (uy) + \frac{\partial}{\partial y} (vy) = 0 \qquad [19]$$

The analysis, which then becomes a little more difficult, concludes with values of the mixing region velocities in terms of the ratio of core width to mixing region width — d/b . Moreover it is shown by Kuethe that the solution is exactly the same for the initial mixing at the jet mouth, as might be expected, and that even down to a point near the apex, where d/b is 0.04 , the difference between the velocity as calculated by the first

and second methods is never greater than 2 percent.

It is therefore reasonable for all engineering purposes to retain the results of the first method outlined here, and apply them with general precaution to all cases of jet mixing in which the entrained fluid velocity is relatively small. The method is not however, universally applicable to to all cases of single stage ejectors, since the analysis has been made on the assumption of equal and constant density of the two fluids. Even in the case of an air ejector operating from 65 psig. to 3.3 psia., that is with a pressure ratio of 24.0 , with an efficiency of 70 percent, the exit temperature of the jet will be 0.61 of the initial total temperature, and the density will therefore be that same fraction of the entrained air density, assuming the same total temperature. Although no definite limit has yet been set, it is pointed out by Goff and Coogan* that a density ratio of 0.37 precludes reliable results for the mixing region.

---

* J. A. Goff and C. H. Coogan, " Some two dimensional aspects of the Ejector Problem". A. S. M. E. Transactions, 1942, vol. 64, pp A151-A154.

CHAPTER 4

Apparatus

The test equipment comprises an air ejector in which as many of the physical dimensions as possible, are variable. The primary nozzle is shown in cross-section in Figures 9 and 11, and the internal profile is given in table 3 on page 26. It is designed for operation with air at 65 psig. and a back pressure of 3.3 psia., consuming the full capacity of the available air compressor. The latter is a reciprocating experimental steam driven compressor delivering 0.126 lbs./sec. at 80 psig. The secondary fluid is also air, drawn in at room conditions, and reduced in pressure as required, by a restricting control valve.

The general layout of the apparatus is shown in Figures 10 and 12, in which the high pressure supply enters at the left, and passes a control and spill valve, metering orifice and through the primary nozzle. The secondary air is drawn in through a flared entrance, metering orifice and control valve into the secondary nozzle. The flange system permits the secondary nozzle to be attached directly to the tee, or suitably spaced from it as shown. The mixing section is also made in tongue and grooved lengths to be extended as required, by loosening the securing nuts on the diffusor flange and inserting the extra length of section required.

The tests were limited to the one primary and secondary nozzle, with the distance from primary nozzle exit to secondary throat variable from zero to six inches, and the mixing section variable from zero to one and three-quarters of an inch.

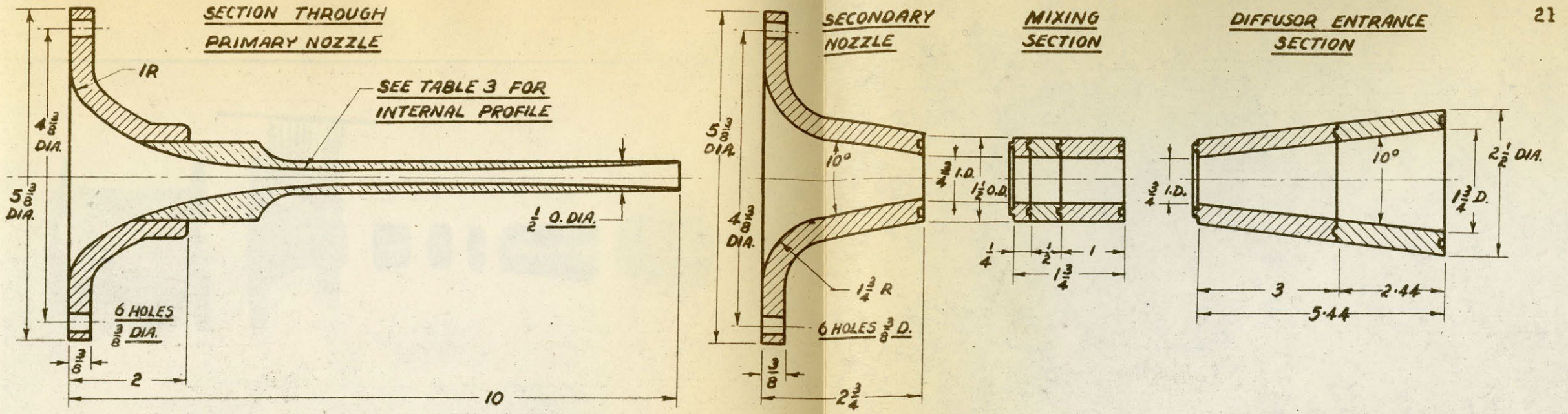

FIG. 9 – SECTIONAL VIEW OF NOZZLES AND MIXING SECTION

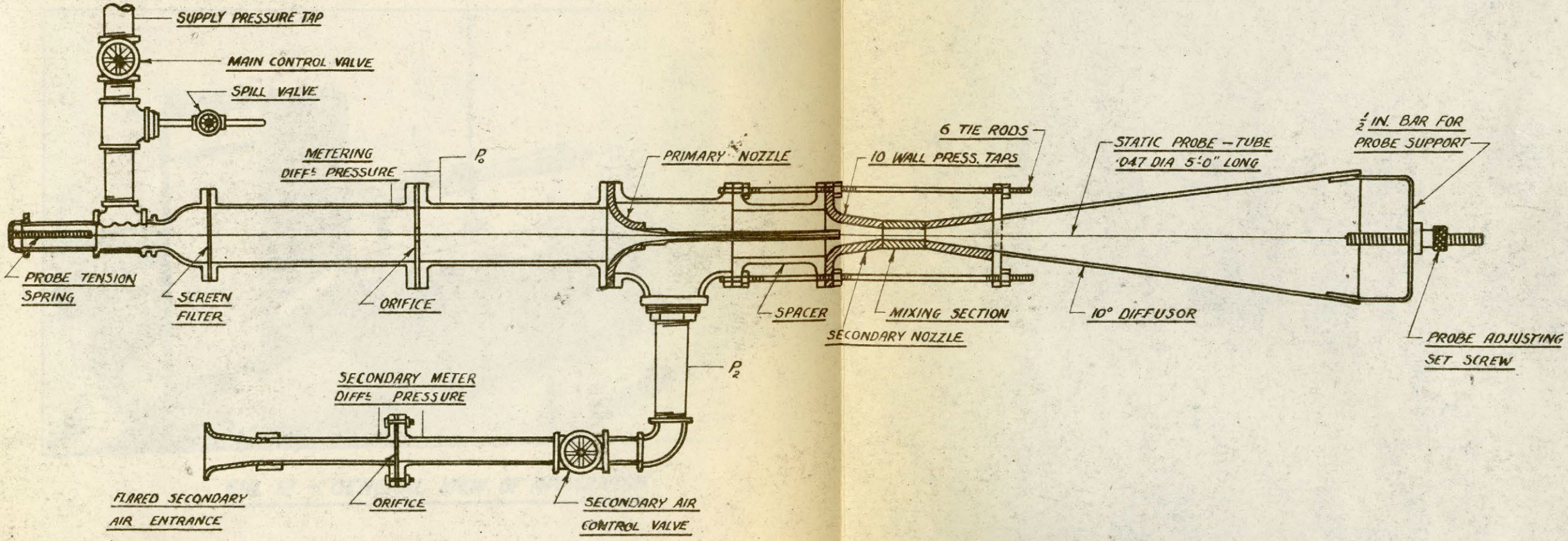

FIG. 10 – GENERAL VIEW OF EJECTOR TEST APPARATUS

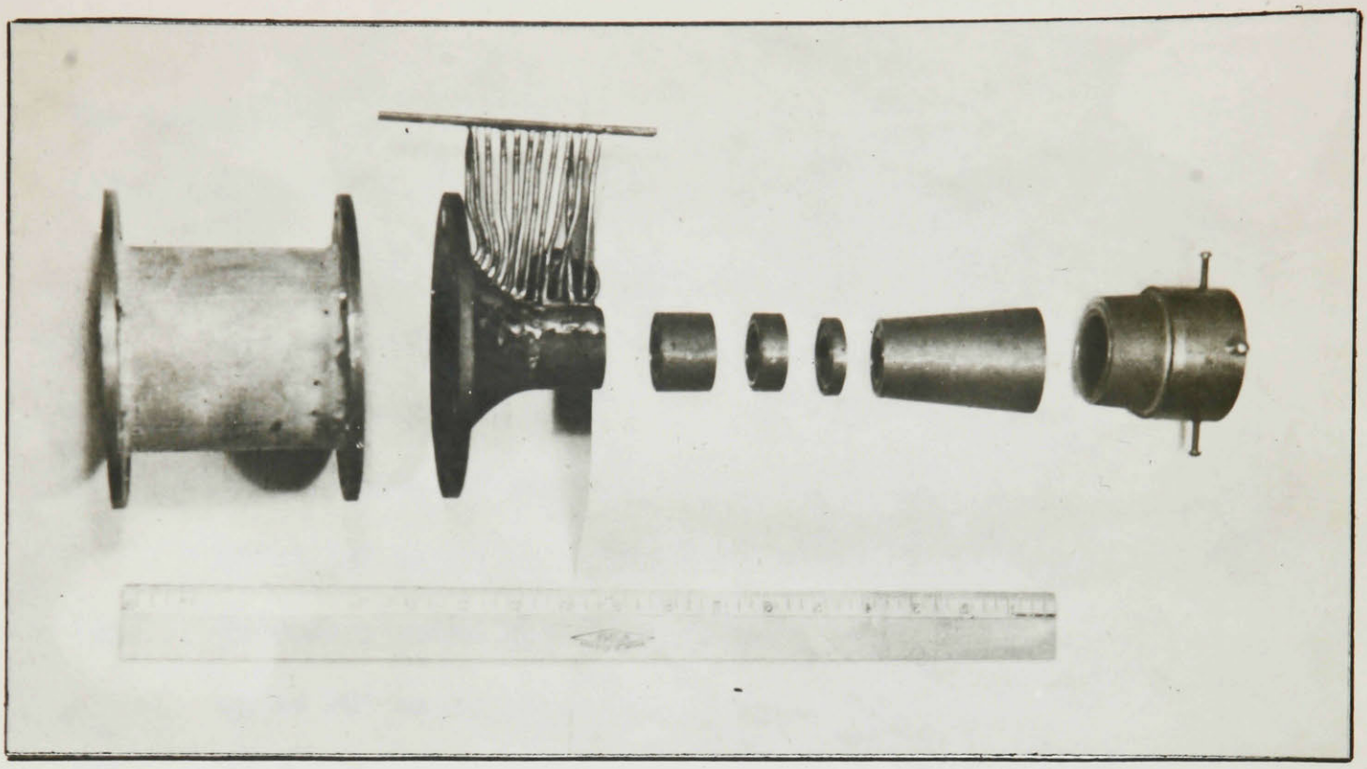

FIG. 11 - VIEW OF NOZZLE ASSEMBLY

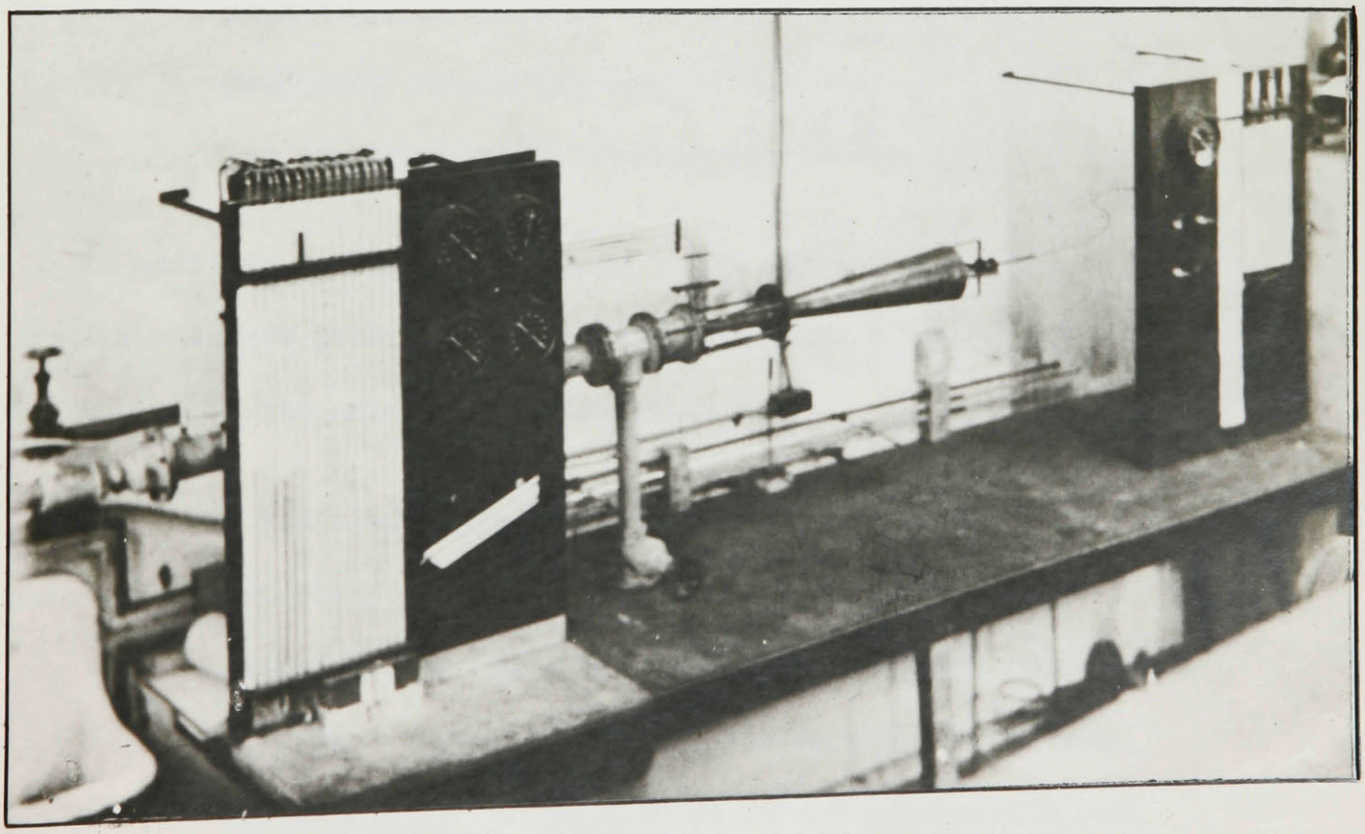

FIG. 12 - GENERAL VIEW OF APPARATUS

The instrumentation consisted of the following readings:-

(1) Main air supply pressure, ahead of the main valve, range up to 100 psig.

(2) Upstream total pressure on the primary nozzle, P_o, kept at 65.3 psig.

(3) Primary meter differential manometer reading, about 15" water on an orifice of 7/8" diameter.

(4) Secondary meter differential manometer reading up to 20" water on an orifice of 1" diameter.

(5) Secondary air supply pressure P_2, reading up to 29" mercury vacuum.

(6) Primary stream temperature to read T_o and maintained at 80.0°F.

(7) Secondary stream temperature to read T_2 (room air temperature) maintained within 2 degrees of T_o.

In addition to the above values which were obtained for each test, a static pressure probe on the centerline and a series of wall pressures were taken for one nozzle position, as follows.

(8) A stainless steel tube of 0.047" outside diameter and about five feet long was stretched along the centerline of the pipe, nozzle and diffusor between a tension spring at one end and an adjusting screw at the other. This is shown in the general diagram, Figure 10. It was found necessary to locate the

Testing Procedure

The apparatus was operated throughout with air for both media at the same temperature, 540° Rankine, within a deviation of two degrees or 0.4%. The primary actuating pressure was maintained at 65.3 psig (80 psia) within 0.1 psi. (0.12%) and the diffusor discharge pressure was at all times the prevailing barometric value. In addition since only one pair of nozzles were used throughout the tests, the cross-sectional area ratio remained constant. This left the following four variables:-

(1) Projection Ratio — the distance from the primary nozzle exit to the upstream end of the parallel mixing section, expressed in secondary throat diameters.

(2) Mixing Length Ratio — the length of the parallel mixing section, expressed in terms of the transverse diameter.

(3) Mass Flow Ratio — adjusted in conjunction with the secondary inlet pressure P_2 by means of the secondary control valve.

(4) Secondary Inlet Pressure — reduced automatically as the secondary mass flow was reduced.

By means of the spacers and extensions described previously it was possible to select a range of projection ratios and mixing length ratios as tabulated below, (page 26).

This provided a total of twenty different geometric arrangements of the ejector, by combination in sequence, of the smaller parts. For each

TABLE No. 2 — PRINCIPAL RATIOS AND DIMENSIONS					
Projection Length Projection Ratio	5/16 0.417	1 3/4 2.42	2 3/4 3.75	4 1/4 5.75	5 3/4 7.75
Mixing Length (ins.) Mixing Ratio	0 0	1/2 0.666	1 1.33	1 3/4 2.33	

arrangement the remaining two variables listed above were altered dependantly to obtain the performance of the ejector, that is, mass flow versus induced pressure.

After obtaining one complete set of readings at the lowest projection ratio, the centerline probe was inserted, and the wall pressure taps were drilled, to investigate the mixing process more thoroughly. One set of performance characteristics was obtained with these for a projection ratio of 2.42 . However since it was necessary to disconnect the probe adjusting screw, static centerline probe and diffusor in order to add each additional length of mixing section, it was decided to omit the probe for the remaining three projection ratios.

TABLE No. 3 — INTERNAL PROFILE OF PRIMARY NOZZLE											
Distance Downstream (ins.)	0	1.00	2.00	3.00	4.00	5.00	6.00	7.00	8.00	9.00	10.0
Diameter (ins.)	5.37	·400	·343	·325	·314	·312	·318	·330	·358	·413	·614

CHAPTER 5

Results and Discussions

Performance Curves

A complete tabulation of the entire performance characteristics is made in table 4, on page 28. From these a series of curves has been compiled, to show in graphical form, the variation of induction pressure with mass flow for each projection ratio, as Figure 13 on page 29. In addition these curves have been cross-plotted to show the variation of induction pressure with projection ratio, for each mass flow, as Figure 14 on the same page. Each of these graphs shows also the effect of increasing the length of mixing section, on the performance of the ejector.

With reference to the first figure, it will be seen that in all cases, an increase of the secondary mass flow demands an higher absolute induction pressure, and consequently, as might be expected, higher vacua can be obtained only at relatively low mass flow ratios. It is also apparent that for a projection ratio of 3.75 or less, the performance is improved by a longer parallel mixing section, with 2.3 diameters inadequate for mixing at the shortest projection. However for a projection of 5.75 and greater, the reverse effect is noticed, and it is desirable to reduce the parallel section for best performance in this case.

Upon examination of Figure 14, the same results are again demonstrated in another form, and in addition it will be noticed that the lowest ordinate (highest vacuum) progresses to the right, that is, to higher projection ratios, as the mass flow is increased.

TABLE No. 4 — GENERAL SUMMARY OF RESULTS

Projection Ratio	Mixing Length Ratio	VALUES OF P_2/P_5 IN TABLE				
		$\bar{m} = 0$	$\bar{m} = .15$	$\bar{m} = .30$	$\bar{m} = .40$	$\bar{m} = [\ ]$
0.417	0	0.700	0.770	0.835	0.930	0.973
	0.66	0.608	0.725	0.813	0.923	0.974
	1.33	0.503	0.681	0.800	0.930	[.45] 0.974
	2.33	0.329	0.598	0.759	0.917	0.974
2.42	0	0.400	0.645	0.780	0.800	0.910
	0.66	0.335	0.585	0.740	0.790	0.910
	1.33	0.263	0.610	0.671	0.763	[.55] 0.910
	2.33	0.180	0.453	0.575	0.676	0.910
3.75	0	0.424	0.493	0.606	0.714	0.800
	0.66	0.340	0.452	0.582	0.714	0.862
	1.33	0.256	0.420	0.527	0.720	[.52] 0.870
	2.33	0.180	0.417	0.524	0.710	0.870
5.75	0	0.322	0.483	0.598	0.800	[.51] 0.967
	0.66	0.396	0.490	0.652	0.847	[.48] 0.954
	1.33	0.440	0.497	0.652	0.860	[.46] 0.974
	2.33	0.465	0.491	0.655	0.893	[.45] 0.973
7.75	0	0.732	0.800	0.867	0.977	
	0.66	0.745	0.817	0.860	0.980	
	0.33	0.750	0.806	0.816	0.980	
	2.33	0.750	0.813	0.839	0.980	

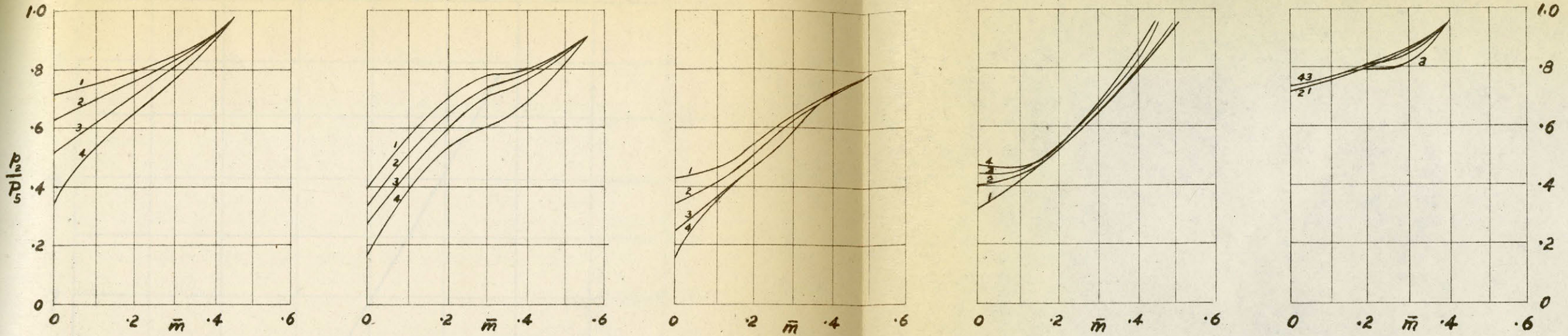

FIG. 13 – GRAPHS OF P_2/P_5 VS. MASS FLOW RATIO

1 – MIXING LENTH RATIO 0
2 – " " " 0.66
3 – " " " 1·33
4 – " " " 2·33

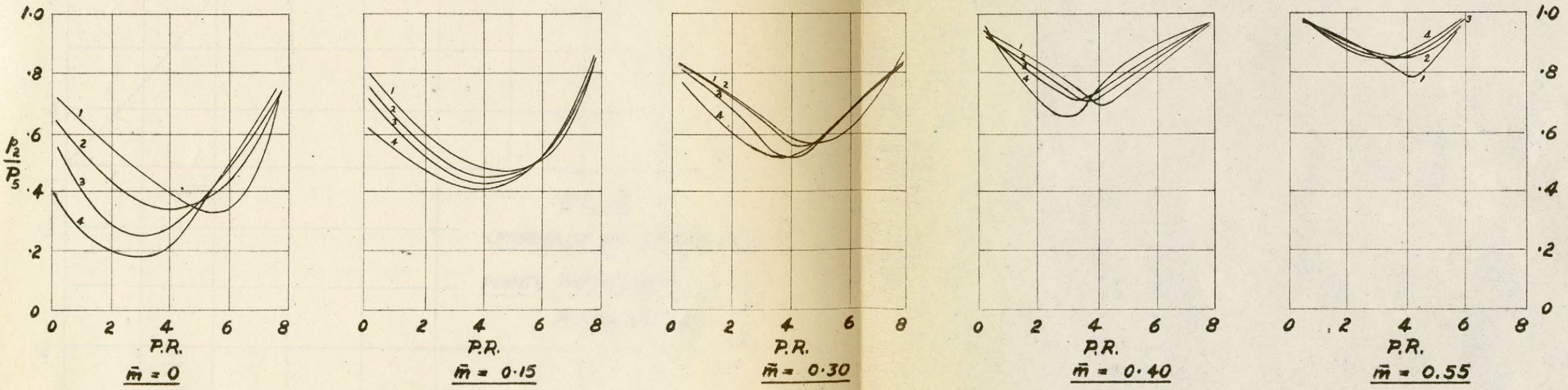

FIG. 14 – GRAPHS OF P_2/P_5 VS. PROJECTION RATIO

1 – MIXING LENGTH RATIO 0
2 – " " " 0.66
3 – " " " 1.33
4 – " " " 2.33

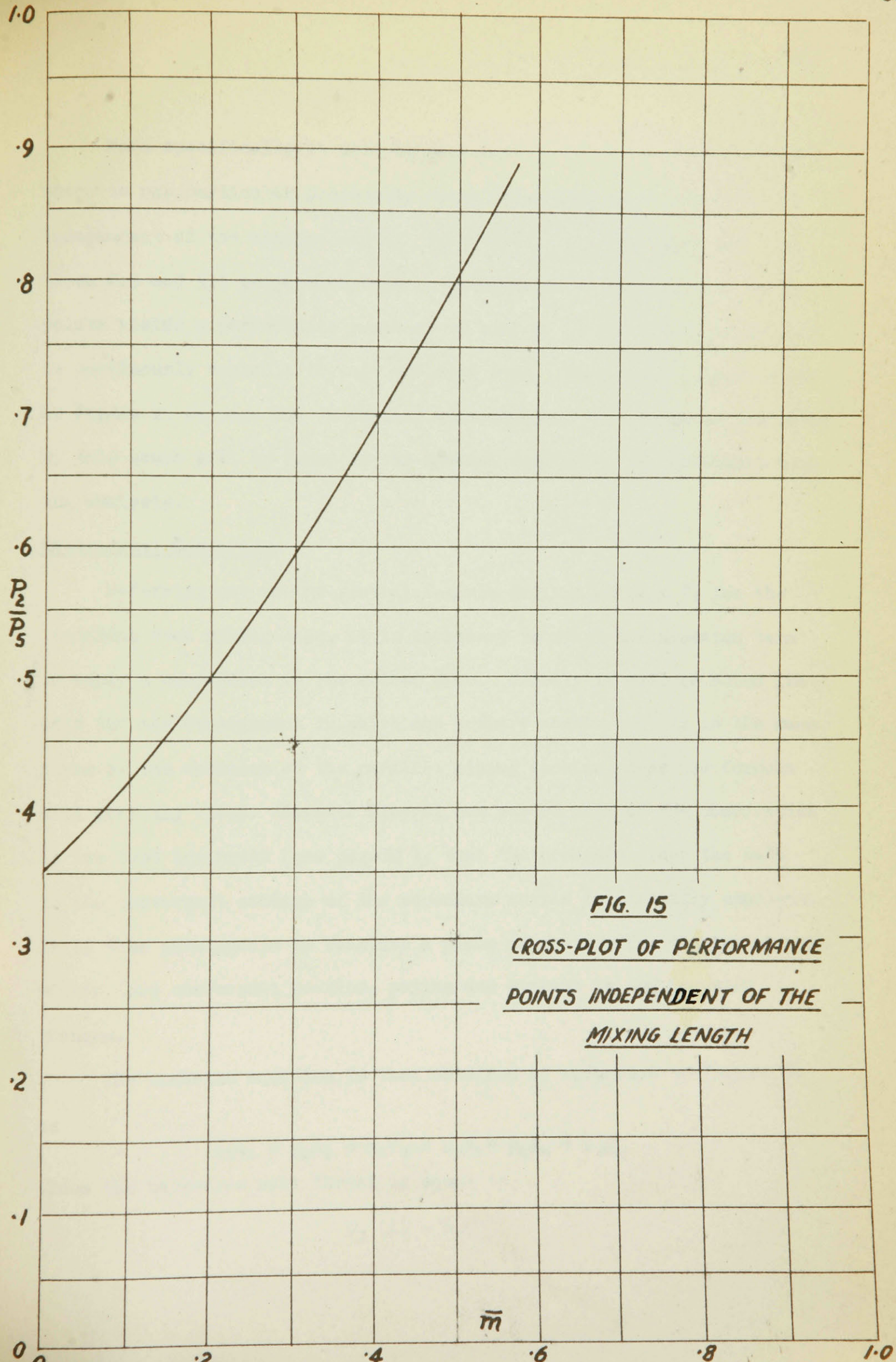

FIG. 15

CROSS-PLOT OF PERFORMANCE POINTS INDEPENDENT OF THE MIXING LENGTH

More specifically it will be seen that for each mass flow ratio, there is one particular projection ratio for which the performance is independent of the mixing length. The abscissa of this point lies between 3.5 and 5.5 projection ratio. In addition a cross-plot of these points yields a performance curve of an ejector in which the projection is continously variable to suit the mass flow. This graph is presented as Figure 15 on page 30. A further discussion of the phenomena indicated by this graph will be found in the section devoted to the turbulent mixing analysis.

Theoretical Comparison

Referring now to the general formula derived on page 7, for the constant area mixing case, it is necessary to adapt the momentum term to apply a comparison to the actual case. Firstly it will be noted that only for the arrangement in which the primary nozzle exit is in the same plane as the entrance of the parallel mixing section, does the formula hold strictly true. However liberal use may be made of the observation in the test equipment (see page40), that the pressure along the wall in the convergent section of the secondary nozzle is virtually constant. It is then permissable to consider a plane of meeting for the two streams within this convergent section, paying due respect to the momentum changes.

The momentum equation is then obtained by reference to Figure 16 as

$$p_1A_1 + p_3A_3 + m_1V_2 + m_3V_3 = p_4A_4 + m_4V_4$$

since the backwards wall thrust is equal to

$$p_3 (A'_3 - A_3)$$

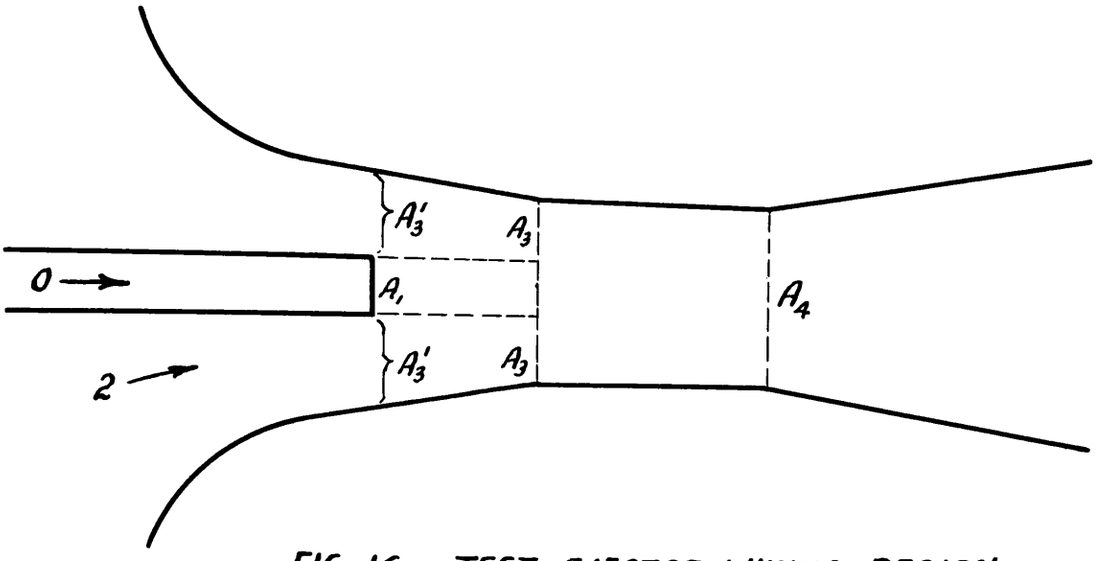

FIG. 16 - TEST EJECTOR MIXING REGION

Again in the test ejector, the primary nozzle was designed for a back pressure of 3.3 psia. and exit Mach number -- i.e. ratio of local stream velocity to local sonic velocity -- of 1.8. After determination of its efficiency it may be shown that provided the back pressure is less than 16.8 psia., the actual back pressure is reached from the value of 3.3 through a series of oblique shock waves or Prandtl-Meyer deflections . Hence the terms p_1A_1 and m_1V_1 remain constant for a fixed value of P_o there being however, losses after the plane A_1, which are considered as part of the mixing process. There are also losses incurred due to the turbulent mixing of the two streams and their relative shearing. For purposes of simplicity all the losses occurring in the process may be expressed as a function of the mean relative dynamic head, as K, where

$$K = \frac{1}{2} k \left\{ \frac{m_1\rho_1 + m_3\rho_3}{m_1 + m_3} \right\} (V_1 - V_3)^2 (A_1 + A_3)$$

and where "k" is the loss factor, or proportion of losses.

By assuming the values of P_2 and a range of mass flows for each, it is possible to find all the necessary constants to solve for V_4 in the revised form of equation [12], Chapter 1.

$$\left[1 - \frac{R}{2Cp}\right]V_4^2 - \left[m_1V_1 + p_1A_1 + m_3V_3 + p_3A_3 - K\right]\frac{1}{m_4}V_4 + RT_4 = 0$$

by selecting suitable ranges for "k". The velocity at V_4 will in nearly every case, be supersonic, and consequently there will follow at section 4, either a normal or oblique shock wave, or a supersonic diffusion with corresponding contraction of the flow. It is debatable as to whether the flow would of its own accord choose a profile which would achieve this letter effect.

Furthermore as the activating fluid leaves the primary nozzle exit at a Mach number of 1.8, two pronounced effects take place. The jet, which is at a static temperature of about 330°R is mixed with air whose temperature is virtually 540°R, tending to increase greatly the sonic velocity in the stream and therefore to reduce the Mach number. In addition, despite the divergence of 1.45 increase in area of cross-section for the flow, the turbulence created by the mixing also tends to reduce the Mach number. The net result is that the velocity at section 4 will seldom, if ever, be greater than Mn 1.8.

With these facts in mind it is possible to draw up a general solution to the above equation for V as a function of the second term of the equation, abbreviated as "b", that is

$$b = \frac{m_1V_1 + p_1A_1 + m_3V_3 + p_3A_3 - K}{m_4}$$

Such a graph is plotted in the non-dimensional form of $V_4/\sqrt{T_4}$ as Figure 17 on page 36. It will be noted that real solutions for the velocity are obtained only where

$$b > 2\sqrt{\left(1 - \frac{R}{Cp}\right) RT_4}$$

which is a function solely of the type of gas and the total temperature after mixing, and is completely independant of the parameters of the ejector itself, except as implied in the sonic velocity at that point. Further it will be noted that for each value of "b", there are two corresponding roots of the equation, one representing the supersonic exit to the diffusor and one being subsonic. Upon examining the former it is found that the resultant total pressure after a normal shock wave is within 1.0% of the value calculated from the subsonic root, and that the Mach number after a normal shock wave is exactly that given by the subsonic root. This however does not eliminate the possibility of higher total pressures in the diffusor where oblique shock waves or other discontinuities exist.

Using the dimensions of the test ejector, and by assuming initially the values of P_2 and $\bar{m}$, a corresponding table of values of "b" are obtained, which may then be interpreted into a total pressure at the exit end of the diffusor. These results are entered in table 5 and plotted as Figure 18 on page 37, in the form of P expressed in psia. versus the value of P_2 expressed as a ratio of the atmospheric or "real" P_5 pressure. Where each of these curves intersects the value of 14.7 psi. representing atmospheric discharge, the analytical results are analogous to the ejector tested. A cross-plot of these significant points produces a series of

curves representing the performance of the ejector with four fixed proportions of kinetic energy loss. These curves appear as Figure 19 on page 38 with the corresponding curve of Figure 13 for a projection ratio of 2.42 as a comparison.

The similarity of this analytical work with the general performance curves shows close agreement with the theory. The general slope of both sets of curves is approximately the same and indicates that a fore-shortened mixing length introduces a constant proportion of losses. It may be seen that the losses corresponding to the experimental results, vary from 5 to 25% of the relative dynamic head of the two fluids.

TABLE No. 5 — VALUES OF "b" FOR EJECTOR UNDER TEST

VALUES OF "b" IN TABLE						
P_2/P_5		0.2	0.4	0.6	0.8	1.0
k	$\bar{m}$					
0	0	2209.4	2318.3	2426.9	2535.4	2645.2
	0.15	1946.0	2020.6	2116.5	2208.6	2303.3
	0.30	1801.6	1837.3	1905.2	1982.8	2062.7
	0.40	*		1786.4	1852.1	1923.4
0.1	0	2089.5	2198.4	2307.0	2415.5	2525.4
	0.15	1875.4	1933.2	2019.9	2106.9	2193.9
	0.30			1825.4	1891.9	1961.6
	0.40					1829.7
0.2	0	1969.7	2078.6	2187.2	2295.7	2405.5
	0.15	1804.8	1845.8	1923.4	2005.2	2084.5
	0.30				1801.0	1860.5
0.3	0	1849.8	1958.7	2067.4	2175.8	2285.7
	0.15			1826.8	1903.5	1975.1

* Values not shown in the table are less than 1785.0 poundal units, and therefore yield imaginary roots to the equation.

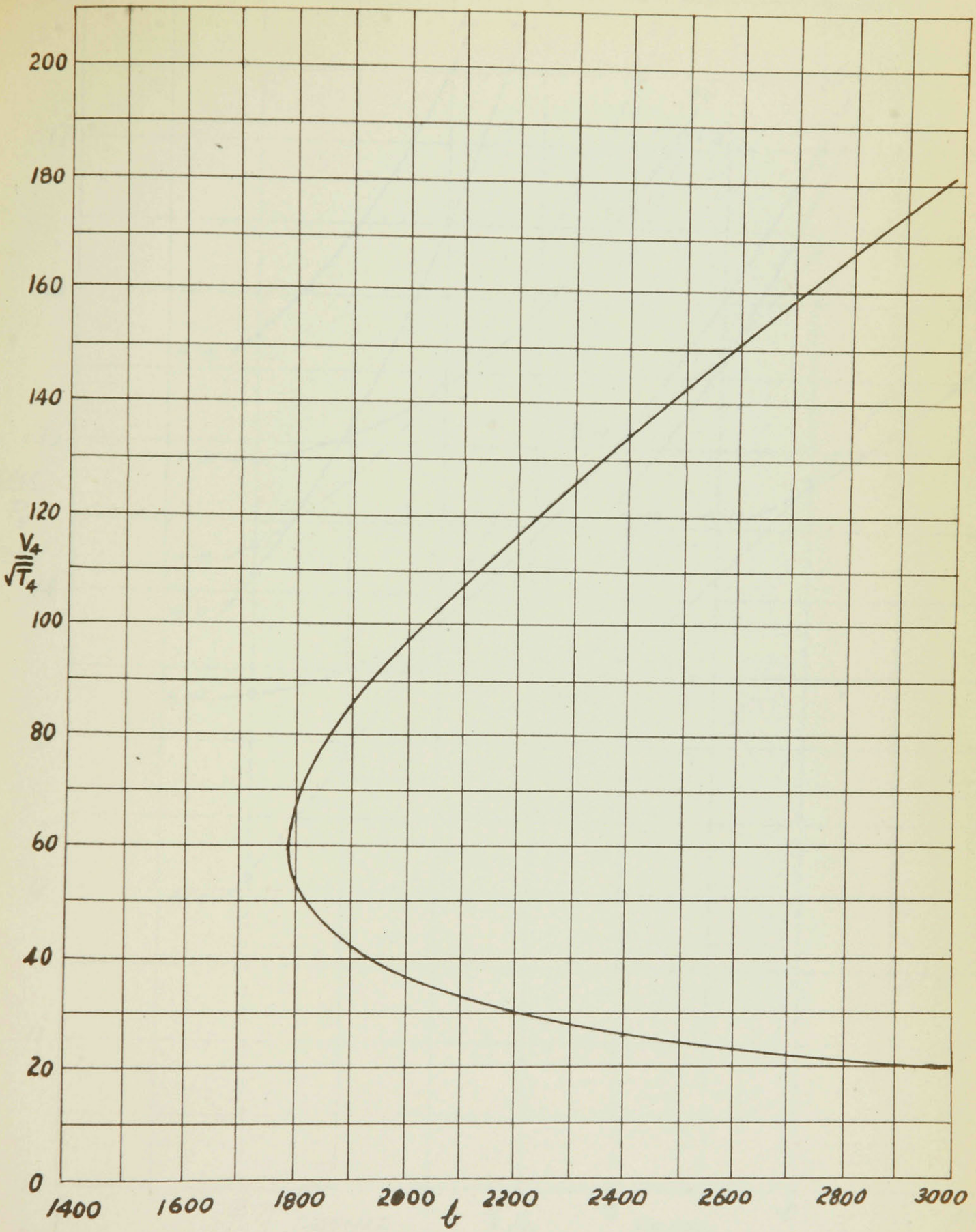

FIG. 17 - GRAPH OF $V/\sqrt{T}$ VS. "t" (IN PDLS.)

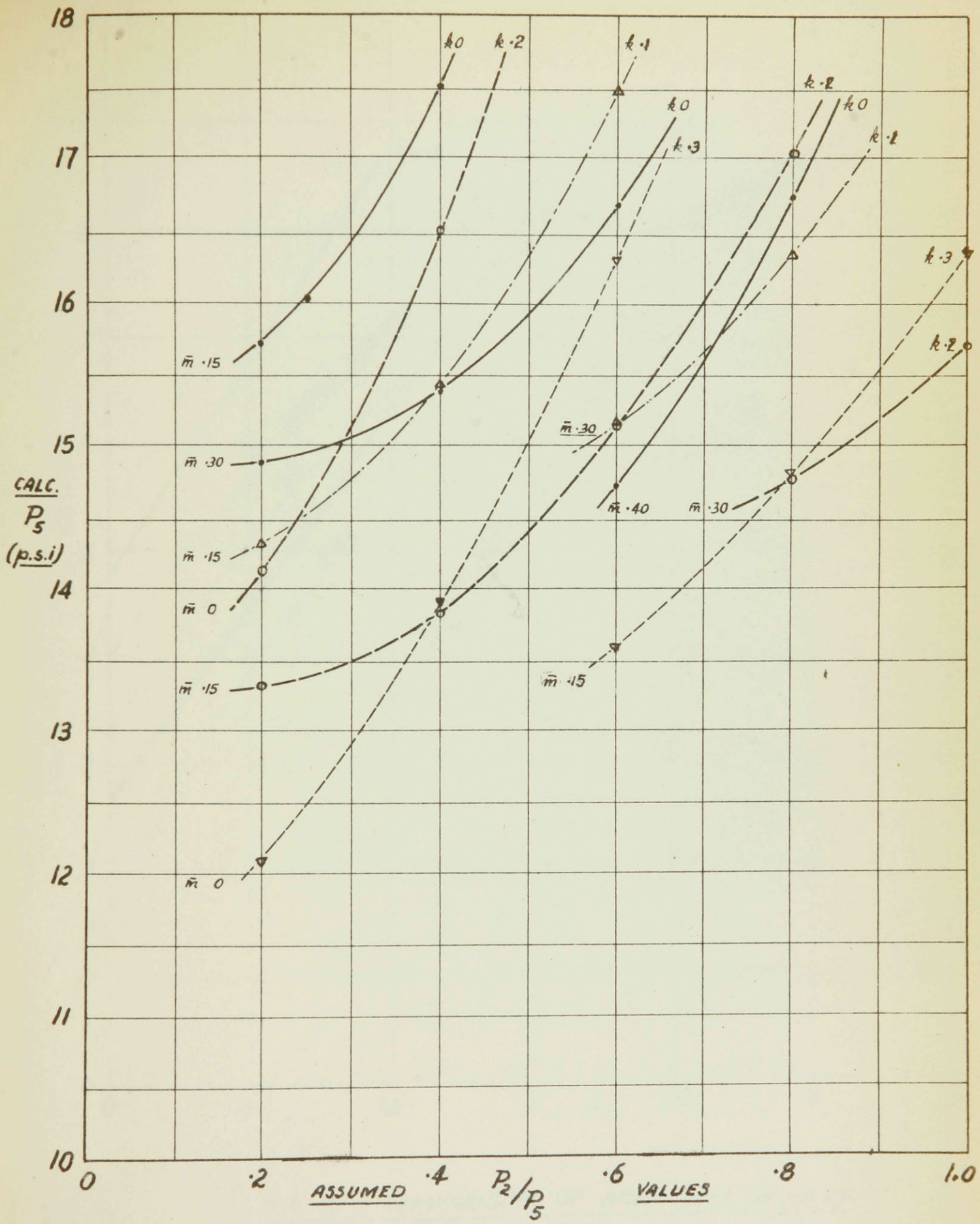

FIG. 18 – GRAPH OF CALCULATED P_5 VS P_2 RATIO.

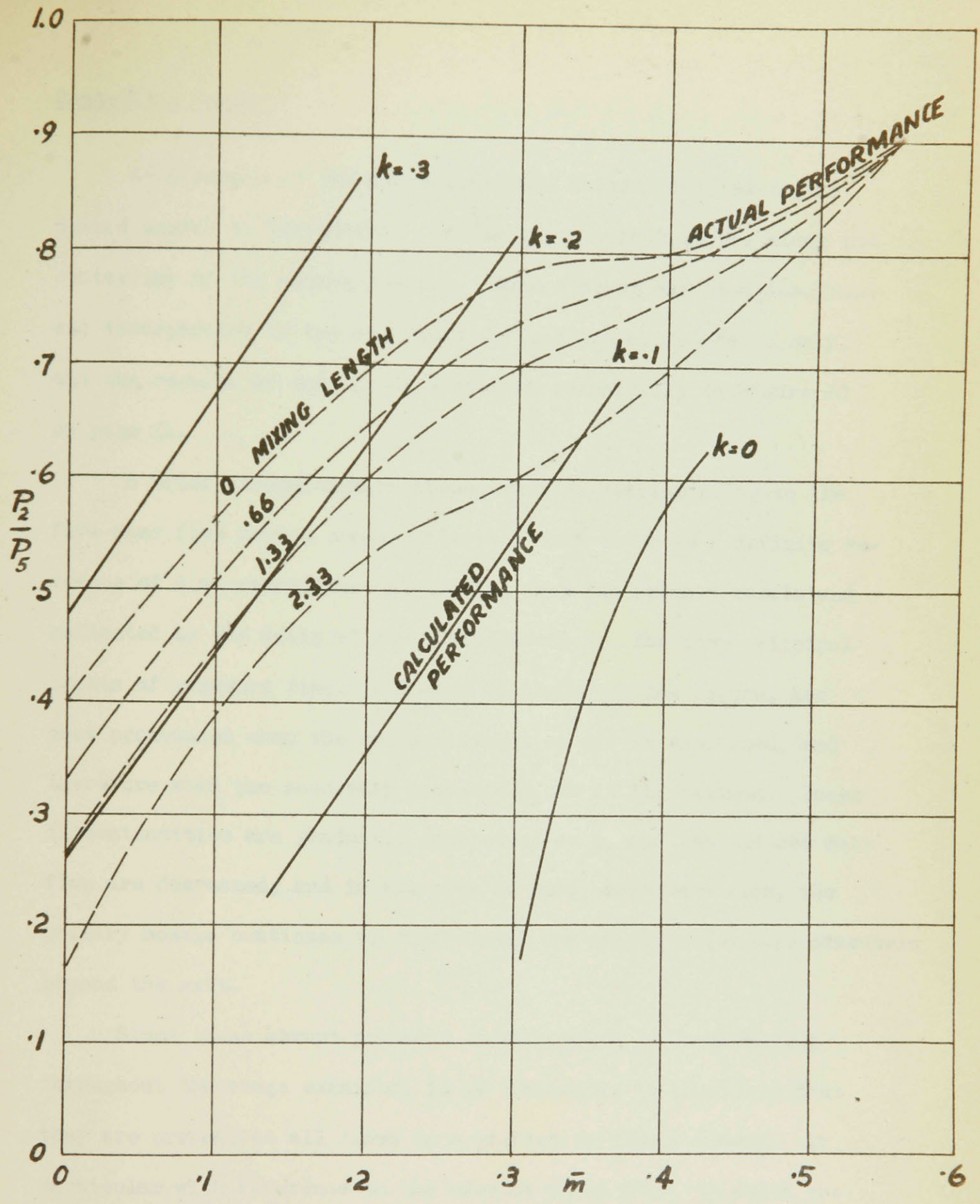

FIG. 19 - COMPARISON OF ANALYTICAL RESULTS WITH ACTUAL PERFORMANCE AT 2·42 PROJ. RATIO

Centerline Probe

As a result of the above mentioned discontinuities it was deemed useful to investigate further the static pressure along the centerline of the mixing chamber. Such a study has been described and incorporated in the equipment for one projection ratio only, and the results of this probe are shown graphically in Figure 20 on page 41.

A brief examination of these profiles corresponding to the five mass flow ratios chosen will show that there is a definite sequence of discontinuities originating from the primary nozzle and reflected by the walls of the mixing section. The five principal crests of pressure rise, indicated by number on the figure, are most pronounced when the maximum amount of air is entrained, and therefore when the secondary pressure p_3 is at its maximum. These discontinuities are gradually suppressed as p_3 and the induced mass flow are decreased, and in the case of zero secondary flow, the primary nozzle continues to over-expand for nearly two nozzle diameters beyond the exit.

Since these abrupt pressure changes occur so pronouncedly throughout the range examined, it is reasonable to postulate that they are present at all times to a greater or lesser extent. In particular with reference to the ejector under test, in which the primary exit Mach number is 1.8, it is improbable that the speed of the stream at section 4 is much above a Mach number of unity after

progressing through such a series of discontinuities. However it is strongly felt that the relative position and intensity of these waves may have much bearing on the performance, especially where, due to a narrow mixing section, these waves are reflected from the walls or turbulent boundary layers.

Static Wall Pressure Taps

The pressures measured at the wall of the secondary convergent section are shown graphically in Figure 21 on page 42. These pressures, taken in conjunction with the centerline probe, reveal that there is little change in the static pressure along the inside surface, except at the first and last points at which taps were placed. The magnitude of the average pressure along this profile is closely equal to that of the induction pressure P_2. The rise of the curves at the downstream end may be attributed to either a partial impact pressure registered from the diffusion of the jet, or the rise in static pressure occurring through an oblique shock wave incident between stations 9 and 10. The higher values at the upstream end can only be explained as due to a leak in the connection, despite exhaustive measures to prevent this. However one general trend is borne out, in as much as no discontinuities are observed at the wall at the highest mass flow, despite the highly irregular pressure profile at the centerline under these conditions. As a result, the observations of this method prove of little value, except as applied to the theory on page 31.

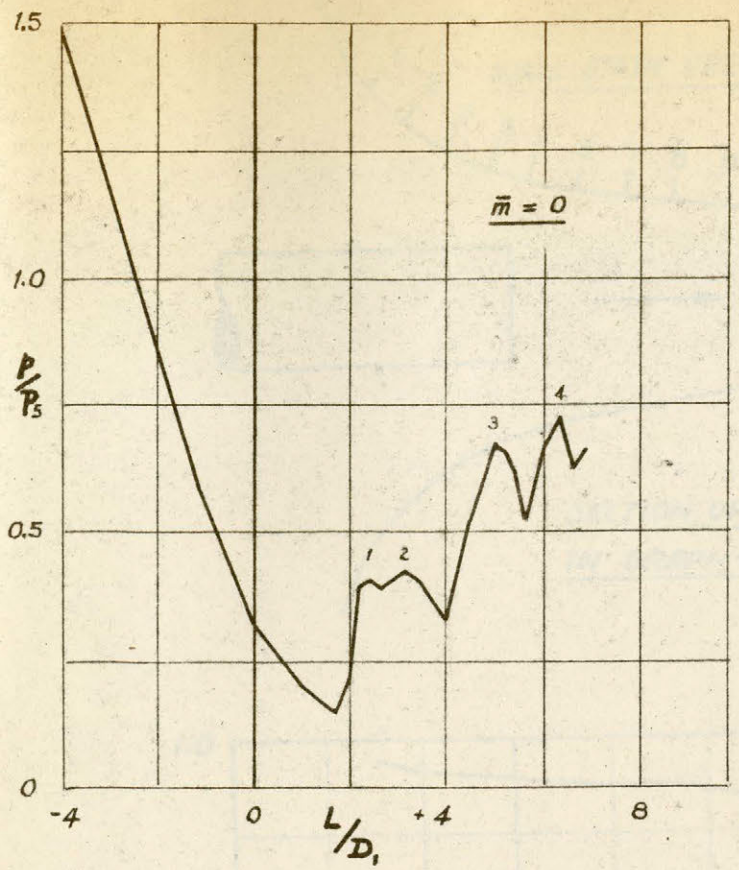

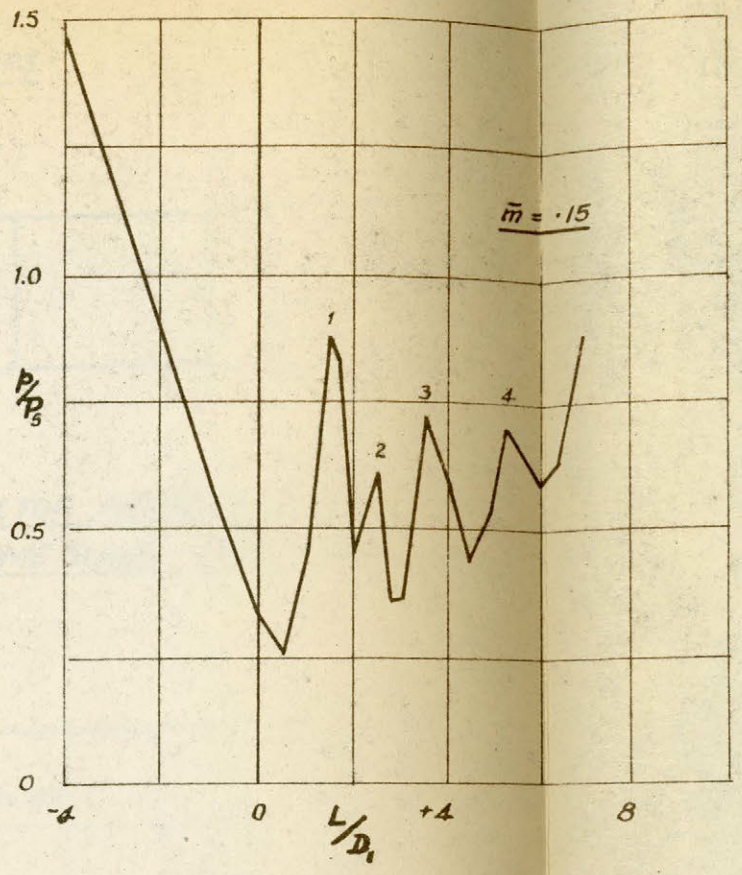

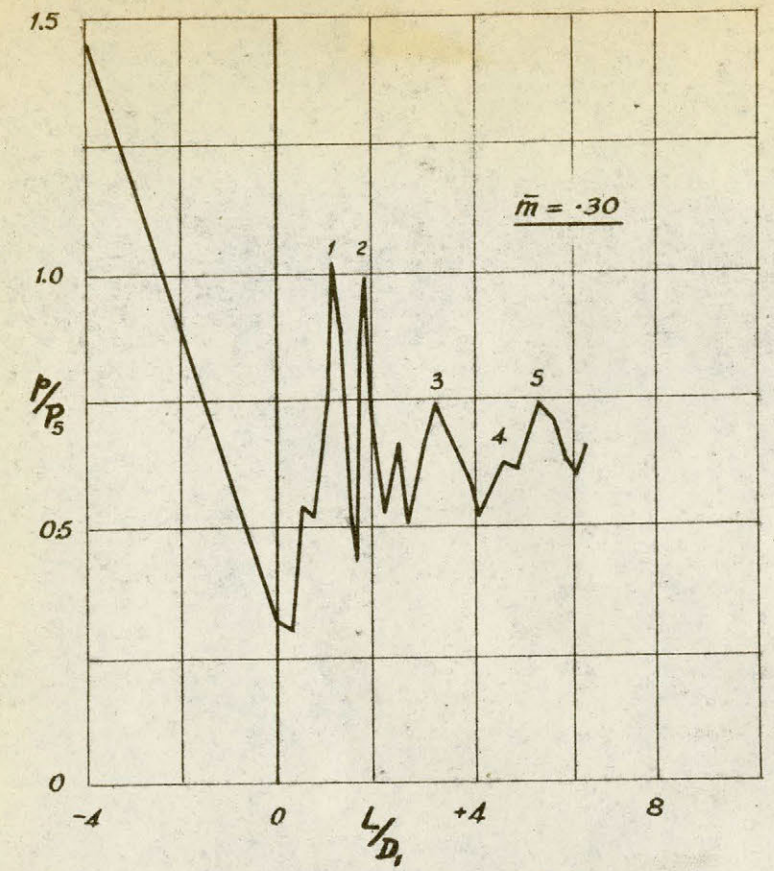

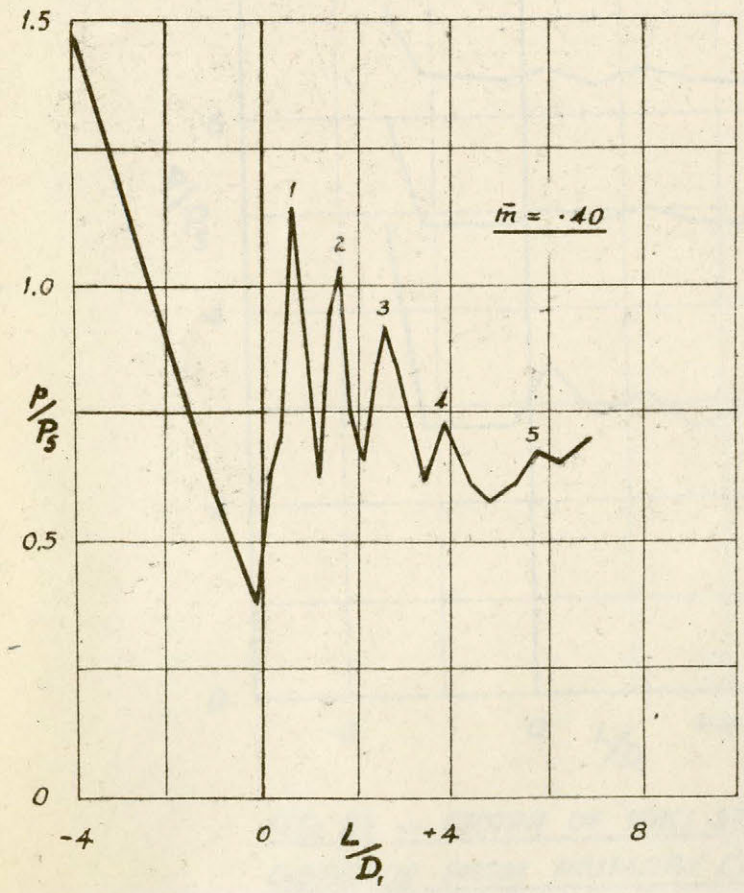

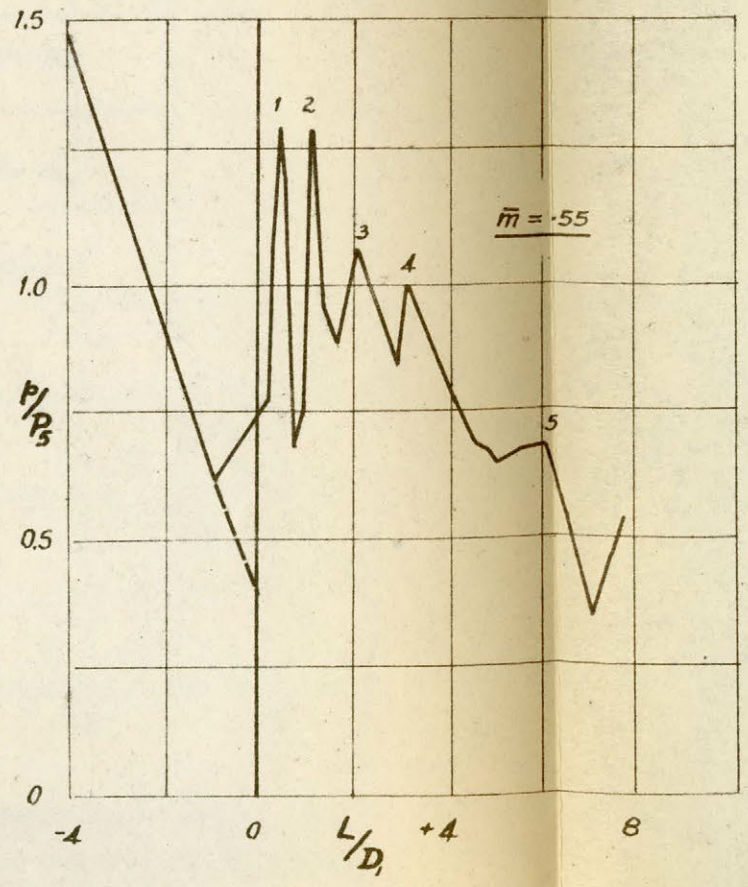

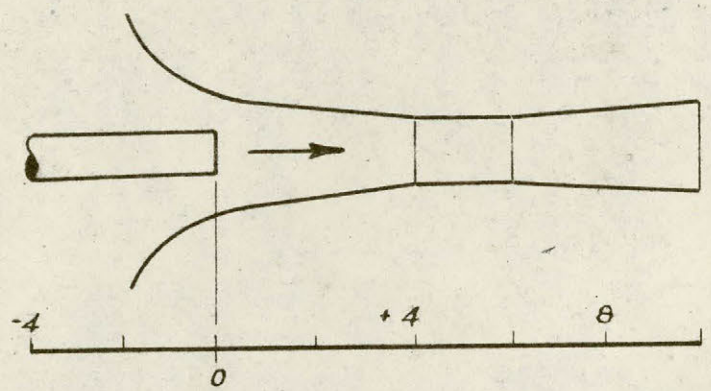

SECTION OF EJECTOR REPRESENTED ON GRAPHS

PROJECTION RATIO = 2·42

MIXING LENGTH RATIO = 1·33

FIG. 20

GRAPHS OF PROBE STATIC PRESSURE RATIO P/P_S vs. DISTANCE DOWNSTREAM FROM PRIMARY NOZZLE EXIT (IN PRIMARY NOZZLE DIAMETERS)

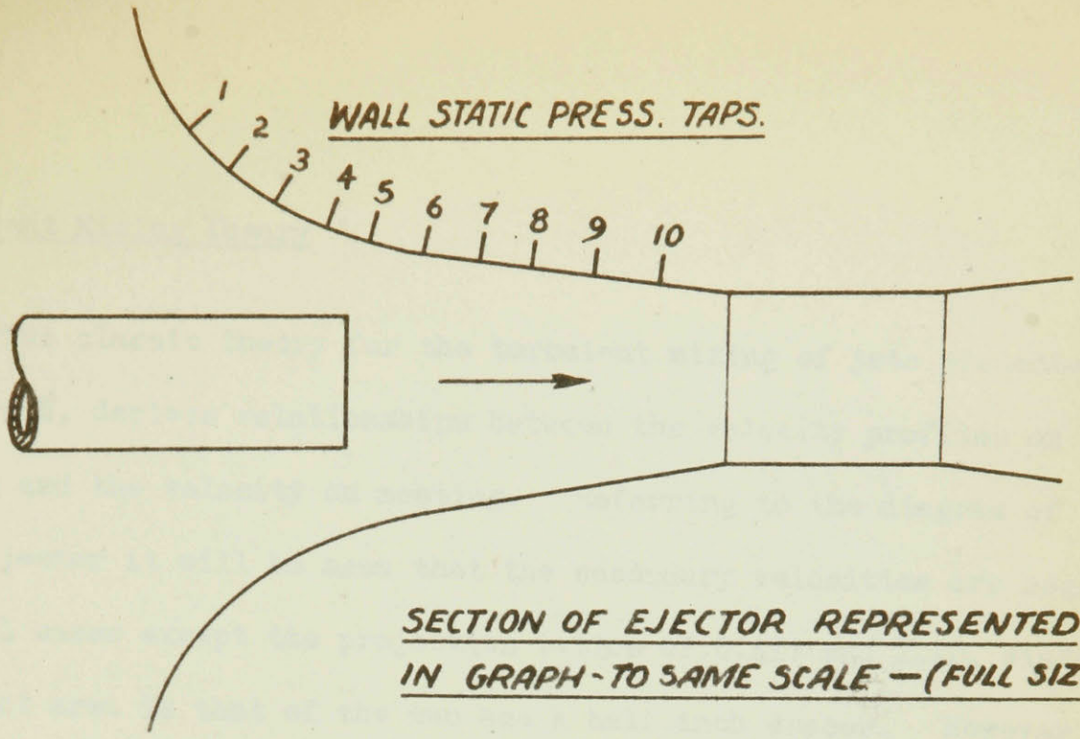

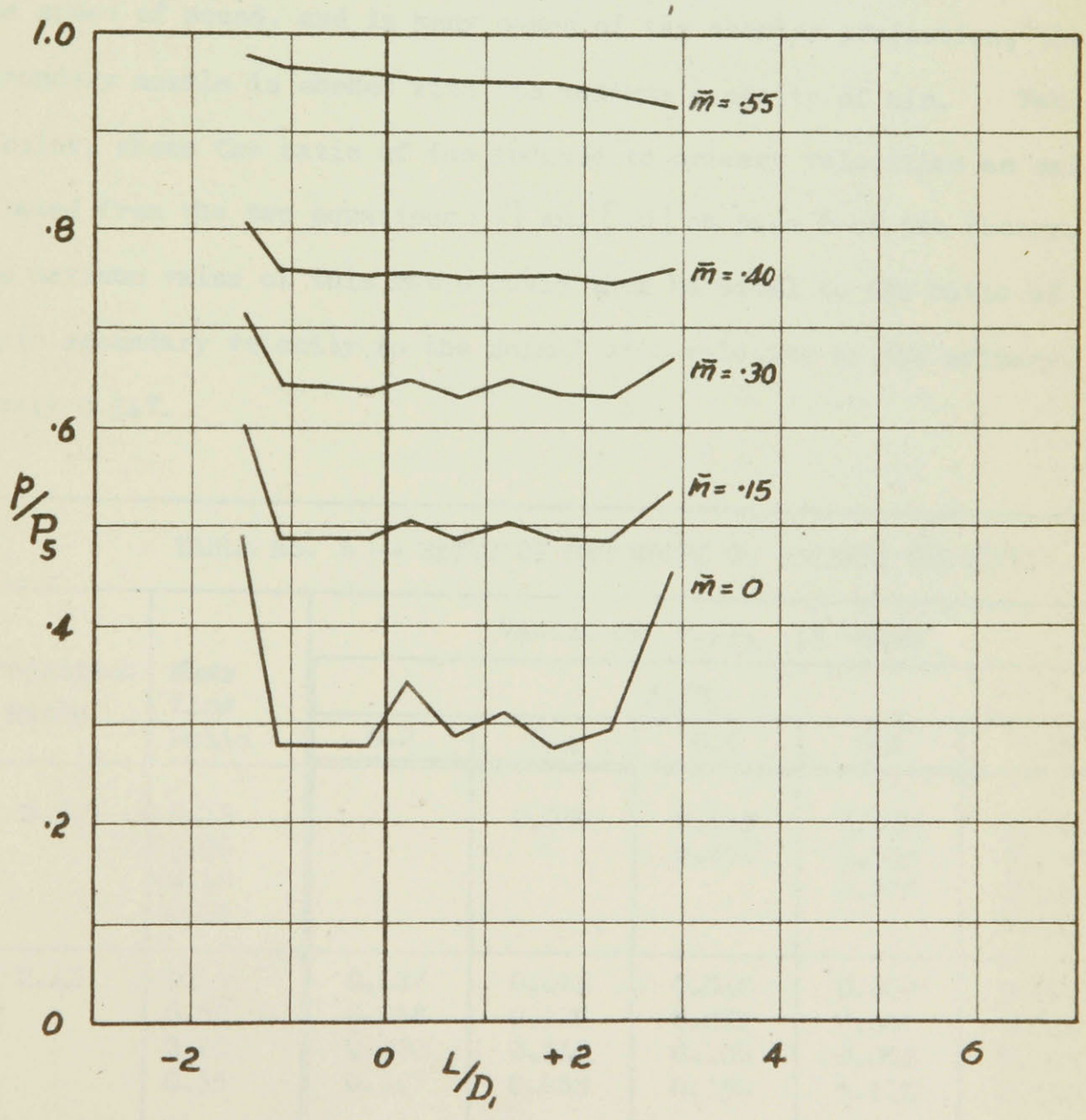

FIG. 21 — GRAPH OF WALL STATIC PRESSURE RATIO VS. DISTANCE FROM PRIMARY EXIT (IN PRIM. NOZZLE DIAS.)

Turbulent Mixing Theory

The classic theory for the turbulent mixing of jets presented in Chapter 3, derives relationships between the velocity profiles on mixing and the velocity on meeting. Referring to the diagram of the test ejector it will be seen that the secondary velocities are negligable for all cases except the projection ratios of 0.417 and 2.42, since the duct area is that of the two and a half inch spacer. However for these two cases the velocity of the induced fluid attains values up to the speed of sound, and in many cases of the shorter projection, the secondary nozzle is choked with its maximum capacity of air. Table 6 below, shows the ratio of the induced to primary velocities as calculated from the two equations [9] and [10] on page 6 of the theory. The maximum value of this ratio would then be equal to the ratio of sonic secondary velocity to the normal exit velocity of the primary, namely 0.547.

TABLE No. 6 — RATIO OF SECONDARY TO PRIMARY VELOCITY

Projection Ratio	Mass Flow Ratio	VALUES OF V_3/V_1 IN TABLE				
		P_2/P_5				
		0.2	0.4	0.6	0.8	1.0
0.417	0.15		0.250	0.160	0.130	0.095
	0.30			0.372	0.250	0.197
	0.40				0.373	0.266
	0.55					0.435
2.42	0.15	0.127	0.063	0.040	0.030	0.024
	0.30	0.258	0.123	0.081	0.061	0.048
	0.40	0.400	0.163	0.109	0.082	0.065
	0.55	0.547	0.238	0.150	0.113	0.090

From these ratios it is now possible to find the corresponding values of η_1 and η_2 in Figure 5, (page 16) and thereby find the increase of radius of the jet per unit length downstream, that is tan θ as defined on page 17. These values of tan θ have been calculated for the complete range of mass flows and pressure ratios and are plotted as Figure 22 on page 46. These curves indicate as might be expected, that as the induced pressure is reduced, the primary nozzle expands into the lower pressure region with a wider angle of divergence. At the same time an increase of the secondary mass flow, tends to reduce this angle by virtue of the fact that the velocities are becoming more nearly equal, and in the extreme case if the two stream velocities were exactly equal there would be no spread of the jet at all.

The analysis of page 18 of the theory introduces the consideration of a point at which the two streams are just mixed uniformly, and beyond which the velocity profile is similar. This point is indicated as "e" on Figure 8. The location of this apex may be found by determination of the length required for the inside boundary of the jet to converge to the centerline, and may be expressed in terms of the primary nozzle exit diameter, as

$$\text{Mixing Length} = 1 / \tan\theta = 1 / \eta_1 \sqrt[3]{2c^2}$$

The values of this mixing length are plotted in Figure 23 against the corresponding induction pressure ratio, and show that the length increases slightly as the induction pressure is decreased. The maximum variation of this length is only between 5.9 and 7.0 primary nozzle

diameters downstream, and is lower at the lower mass flows. These characteristics may be attributed to the fact that as the activating nozzle expands into a lower pressure region, the outside boundary diverges more and the inside boundary must therefore converge less. In addition to this, as the jet is required to diffuse more momentum at the higher mass flows, it must necessarily take a longer mixing length to perform the mixing.

Scale Effect

Attention should be drawn to the fact that all the data and performance characteristics have been derived from the one particular ejector under test. Application of the general trends may be made to other ejectors only with considerable caution. The over all performance will only be the same where the flow is aerodynamically similar in all respects. Such similarity would rarely if ever, be met in practice due to the geometric nature of the apparatus ; an ejector in which every dimension is doubled would require four times as much air in both primary and secondary nozzles, and would have four times the ratio of secondary to primary throat areas. Furthermore, if the angle of divergence in the mixing section were to remain constant, the divergence area ratio for this section would necessarily change. It is for this reason primarily, that individual tests of prototypes of new designs should be made in order to determine within any reasonable margin of accuracy, the performance of an ejector.

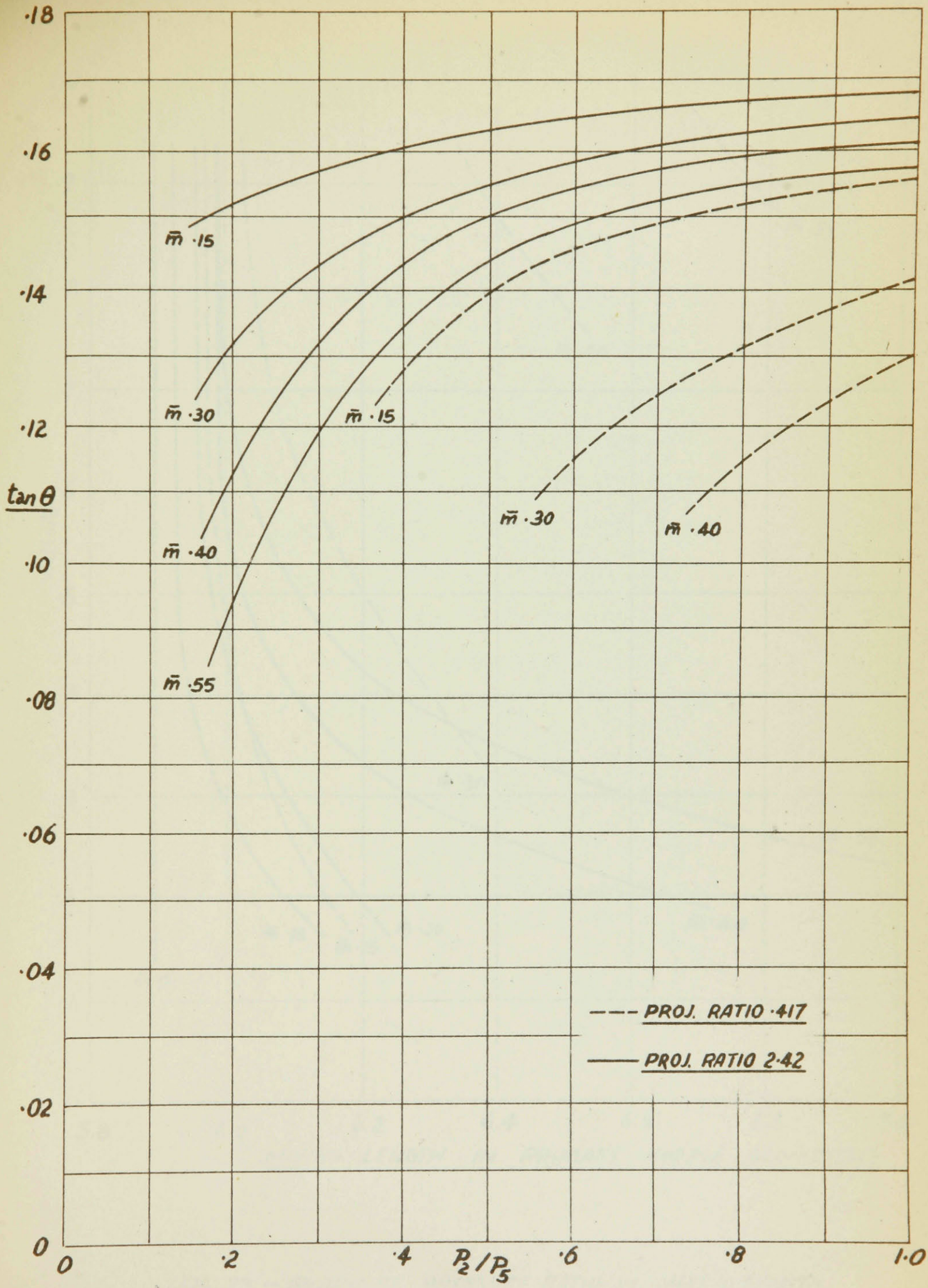

FIG. 22 — GRAPH OF $\tan\theta$ VS. P_2/P_5 —

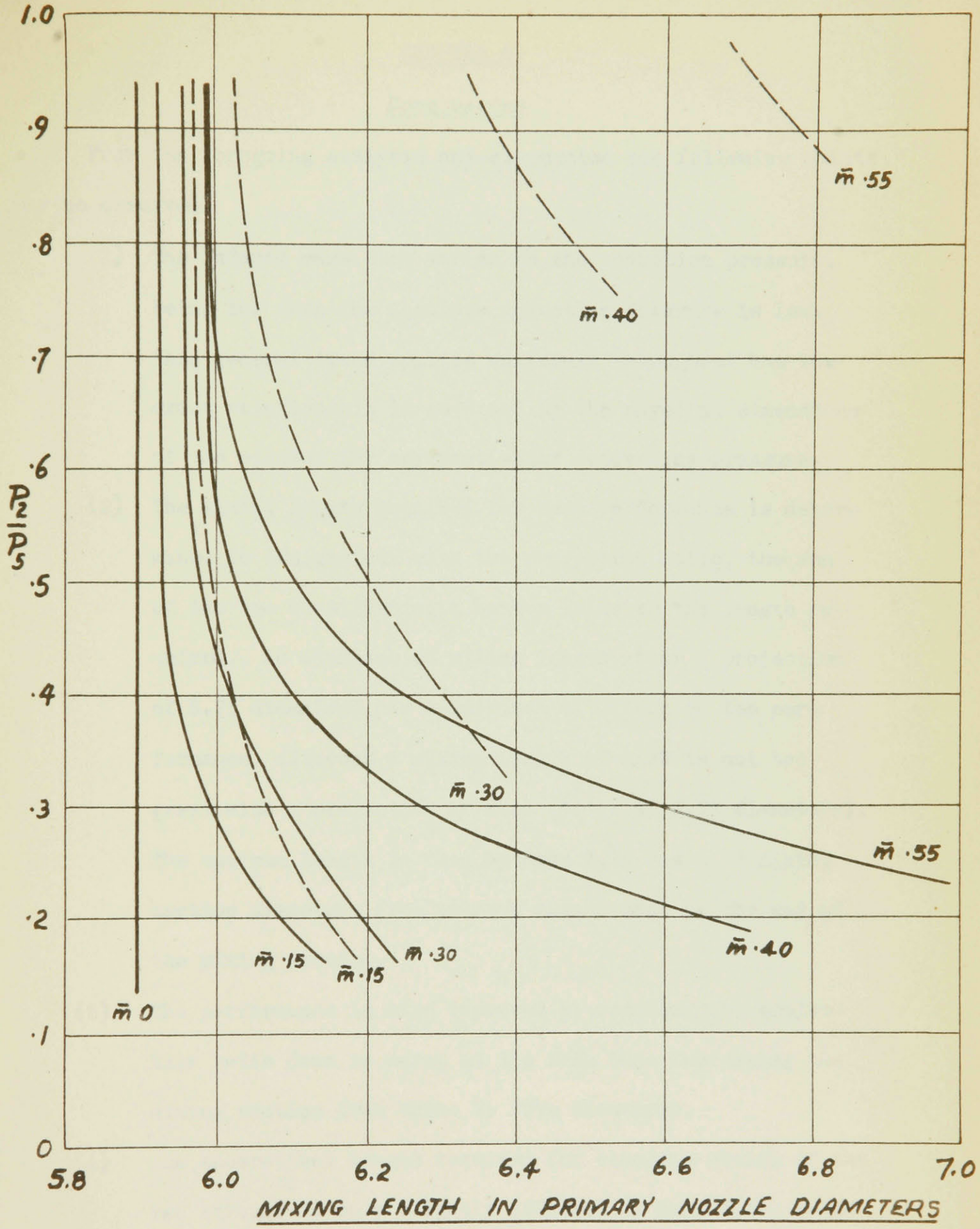

FIG. 23 – GRAPH OF PRESSURE RATIO vs. MIXING LENGTH

– – – – PROJ. RATIO 0.417 ——— PROJ. RATIO 2.42

CHAPTER 6

Conclusions

From the foregoing analysis and discussion the following points may be observed.

(1) The induced mass flow varies as the induction pressure, being low when the absolute induction pressure is low. This general trend applies uniformly throughout but the exact relationship is governed by the physical dimensions of the ejector for any particular activating pressure.

(2) The mixing length required for best performance is determined in conjunction with the projection ratio, the sum of the two constituting a better guide to the length required. An increase of mixing length after a projection of 3.75 diameters has a detrimental effect on the performance, although a mixing length of 2.33 is not too great with a projection of 2.42 (total of 4.75 diameters). The optimum length is then between 3.75 and 4.75 mixing section diameters from primary nozzle exit to the end of the mixing section.

(3) The performance is also improved by reducing the projection ratio down to zero, at the same time increasing the mixing section from three to five diameters.

(4) The theoretical length required for complete mixing of the two streams is only slightly affected by mass flows ratio and induction pressure ratio. The value for this length lies between 5.9 and 7.0 primary nozzle diameters, or 3.95 to 4.7

mixing section diameters. These values compare favourably with the observations of the ejector under test, and with the values given by Kuethe[13] but are appreciably higher than the experimental valves of 1.0 to 1.5 given by Kastner and Spooner[12].

(5) The theory derived in this work for constant area mixing agrees very favourably with the experimental results, showing that losses of up to 25% of the relative dynamic head may be expected in even a well designed ejector. It is also seen that the losses incurred by a fore-shortened mixing length are roughly a constant proportion of the relative dynamic head. However since there is as yet no way of determining these losses without an actual test, it is impossible to do more than hazard an "intelligent guess" at the performance of a new design.

(6) A definite series of pronounced discontinuities is observed for a supersonic primary velocity which are exaggerated by an induction of secondary air. The shape and nature of these shock waves is not readily determinable, but it is recommended that a Schlieren apparatus might be used to good advantage in examining this flow pattern. Investigation with a probe gives results which agree favourably with the observations of Keenan & Neumann[14] in as much as oblique shock waves and thin reflections are apparent.

(7) Geometrical symetry of the flow is virtually impossible to achieve in practice between two different ejectors due to

the scale effect of areas versus length of mixing section.

(8) The present methods of presenting the performance of an ejector have been limited to one particular nozzle area ratio and the characteristics of other area ratios, or divergence angles although similar, may best be determined by experiment.

BIBLIOGRAPHY

1. B.A. BAKHMETEFF, "The Mechanics of Turbulent Flow", published by Princeton University Press 1936.

2. T. BARON and L.G. ALEXANDER, "Momentum, Mass and Heat Transfer in Free Jets". University of Illinois Engineering Experiment Station T.R. No. 5. January 15th, 1950.

3. F.W. BARRY and G.M. EDELMAN, "An Improved Schlieren Apparatus". Journal of Aeronautical Sciences, Volume 15, No. 6, June 1948, p.364.

4. BOSNJAKOIC, "Über Dampfstrablgebläse", Zeitschrift für die Gesante Kälte - Industrie, Volume 43, 1936. pp. 229-233.

5. CHAPLYGIN, "Gas Jets" National Advisory Committee on Aeronautics, Technical Memorandum No. 1063, 1944.

6. D.R. CHAPMAN, "Laminar Mixing of a Compressible Fluid" N.A.C.A. Technical Note 1800, February 1949.

7. H.G. ELROD, Jr. "The Theory of Ejectors" Annapolis Md. Birmingham Alabama, April 3 - 5 1944. A.S.M.E.

8. G. FLÜGEL, "Berechnung von Strahlapparaten" Forschungsheft 395, Supplement to Forschung auf dem Gebiete des Ingenieurwesens, Ausgabe B Volume 10 - March - April 1939.

9. WALTON FORSTALL, Jr. D.Sc. "Material and Momentum Transfer in Coaxial Gas Streams", M.I.T. Doctor's Thesis June 1949.

10. J.A. GOFF and C.H. COOGAN, "Some Two Dimensional Aspects of the Ejector Problem". Transactions of American Society of Mechanical Engineers, 1942. Volume 64, pp. A151.

11. S. GOLDSTEIN, "Modern Developments in Fluid Dynamics" published by Oxford Clarendon Press, 1938.

12. L.J. KASTNER and J.R. SPOONER, "An Investigation of the Performance and Design of the Air Ejector Employing Low Pressure Air as the Driving Fluid".

13. A.M. KEUTHE, "Investigations of the Turbulent Mixing Regions formed by Jets", A.S.M.E. Volume 57, 1935. p. A-87.

14. J.H. KEENAN and E.P. NEUMANN, "A Simple Air Ejector", Transactions of American Society of Mechanical Engineers, 1942, Volume 64, p. A-75.

15. L. PRANDTL, "Bericht uber Untersuchungen zer ausgebildeten Turbulenz", Zeitschrift fur Angewandte Mathematik und Mechanik, Band 5, Heft 2, April 1925, pp. 136 - 139.

16. E. G. REID, "Annular-Jet Ejectors", N.A.C.A. Technical Note No. 1949, Nov. 1949.

17. R. BOYDS and E. JOHNSON, "The Fundamental Principles of the Steam Ejector", Proceedings of the Institute of Mechanical Engineers, 1941, vol. 145 p. 193, and vol. 146 p. 223.

18. A. STODOLA, "Steam and Gas Turbines", published by McGraw-Hill, 1927, Volume 2 p. 927.

19. W. TOLLMIEN, "Berechnung turbulenter Ausbreitungsvorgange" Zeitschrift fur Angewandte Mathematik und Mechanik, Band 6, Heft 6, December 1926 pp. 468-478.

20. TSIEN, HSUE-SHIEN, "Two Dimensional Subsonic Flow of Compressible Fluids". Journal of Aeronautical Sciences, Volume 6, No. 9, August 1939, pp. 399-407.

21. Th. vonKARMAN, "Compressibility Effects in Aerodynamics", Volume 8, No. 9, July 1941, pp. 337-355.

22. F.R.B. WATSON, "Production of a Vacuum in an Air Tank by means of a Steam Jet". Proceedings of the Institute of Mechanical Engineers, 1933, vol. 124, p. 231.

23. H.W. LIEPMANN and A.E. PUCKETT, "Aerodynamics of a Compressible Fluid" Published by John Wiley N.Y. 1947, for the GALCIT series.

24. F.R. MURRAY, "The Distribution of Temperature and Velocity in a Jet in Still Air and in a Moving Air Stream". Rolls-Royce Experimental Department Report. 26.11.43.

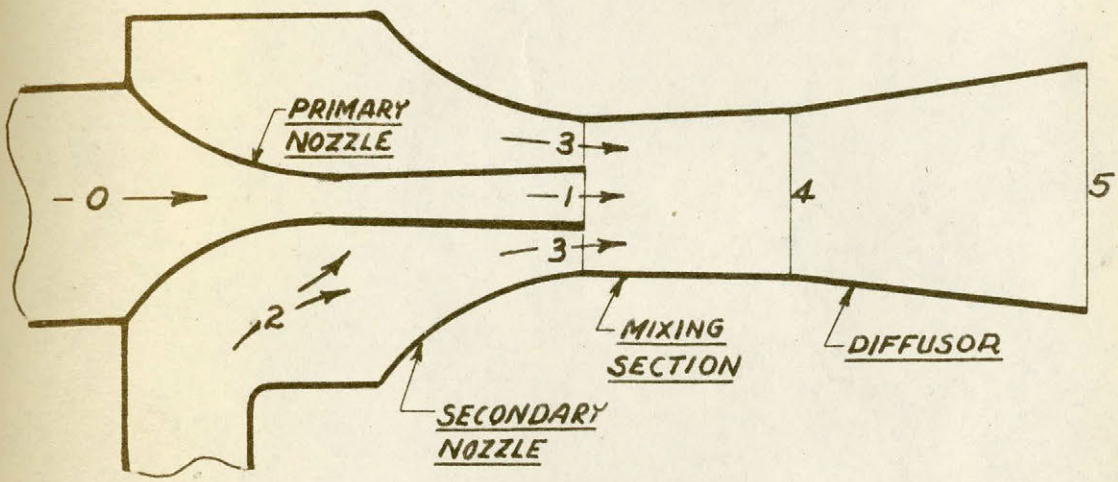

FIG. 1 – CROSS-SECTION OF EJECTOR